DISTRIBUTION OF LUMINOSITY IN ELLIPTICAL NEBULAE[1]

By EDWIN HUBBLE

ABSTRACT

Luminosity-curves for fifteen elliptical nebulae have been derived from *transparency-curves of photographic images* measured with a *Koch registering microphotometer*. The transparencies were reduced to luminosities by means of empirical reduction-curves derived in the laboratory under conditions similar to those affecting the nebular photographs, namely, integrated sunlight, Eastman 40 plates, and X-ray developer.

The curves of luminosity *along various axes* of the different nebulae follow the general trend of the formula

$$\log I = \log I_0 - 2 \log \left(\frac{r}{a}+1\right) ,$$

where I is the luminosity, I_0 the central luminosity, r the distance from the center, and a a parameter varying from nebula to nebula, and, in any one nebula, directly with the radii along which the luminosities are measured.

With r/a as the unit of distance, the curves for all nebulae are parallel and may be shifted into coincidence to form a standard luminosity-curve referring to a standard central luminosity. With these units all *isophotal contours approximate circles*, although for very elliptical or lenticular images the fainter contours are noticeably elongated.

The luminosity formula, derived in the first instance from series of exposures generally up to fifteen minutes, has been further tested in the outer regions by luminosity-curves obtained from seven long exposures, ranging from one to two hours. Moreover, the formula has also been tested at the threshold of the plates, where $\log I$ is constant for a given exposure time, by plotting $\log (r/a+1)$, a function of the measured diameters, against $\log I_0$; and, finally, with the help of the time scale, $\log I_0 = m_1 \log t + C$, by plotting $\log (r/a+1)$ against $\log t$. The *correlations of the three independently observed quantities, diameters, central luminosities, and exposure times*, are supported by long exposures and indicate that the *formula represents the general trend* of the luminosity-curves out to the limit of the measures.

Integration of the luminosity formula leads to the expression for total luminosity:

$$I_t = I_0 a_1 a_2 \left\{ \log \left(\frac{r}{a}+1\right) - \frac{r/a}{r/a+1} \right\} ,$$

where a_1 and a_2 refer to the major and minor axes. Total luminosity thus varies with exposure time in a manner which differs from nebula to nebula. For moderate exposures, however, the formula leads to integrated magnitudes of the same order as those actually measured.

The *corresponding curve* which represents the distribution of luminosity in the nebulae themselves (the three-dimensional bodies) *has been derived* in a manner *analogous to that used in the case of globular clusters*. The mathematical expressions are complicated (probably by the introduction of an empirical formula into an integral equation), but the curve itself exhibits a suggestive similarity, over a considerable range, with that expressing the distribution of density in an isothermal gaseous sphere. The *nuclei* of the nebulae appear to be *relatively more concentrated*, and in the *outer regions* the luminosity *falls off faster than the density*, as would be expected in the case of finite rotating bodies such as the nebulae.

Extra-galactic nebulae, aside from the 2 or 3 per cent of irregular objects, fall into a progressive sequence of types composed of two sections, the elliptical nebulae and the spirals, which merge into each other.[1] The division point is rather well defined, and few transition cases are known.[2] The spiral section is composed of a main sequence of normal spirals and a secondary branch of barred spirals. There is some intermingling of characteristics, and further investigation will be required to determine the full significance of variations in structural detail.

The sequence of elliptical nebulae appears to offer a simpler problem, for the individual objects at any given stage in the sequence are curiously similar. There are, in general, no structural details whatsoever beyond the general appearance of rotational symmetry.[3] From the relatively bright semi-stellar nuclei the luminosity falls away smoothly to undefined borders. As far as the observations can be pushed the diameters increase with the exposure.

The sequence ranges from round images through successive degrees of elongation to the limiting lenticular form with a ratio of axes about 1 to 3. The preponderance of round and nearly round images indicates that we observe the projections of nebulae ranging from globular to lenticular, oriented more or less at random in space. Among the projected images only one pure type can be identified with certainty, namely, the occasional lenticular nebulae, at the very end of the sequence, which happen to be oriented with their minor axes perpendicular to the line of sight. The luminosity distribution in these images is remarkably uniform. As the ellipticities of the projected images decrease, the dispersion in luminosity distribution increases but does not become conspicuous until the round and nearly round images are reached. This suggests a confusion due to random orientation of different forms. When the effects of orientation are eliminated by statistical analysis of extensive material, the nebulae

[1] For the complete classification see *Mt. Wilson Contr.*, No. 324; *Astrophysical Journal*, **64**, 321, 1926.

[2] N.G.C. 4274 and 5750 are good examples. Arms appear to be forming along the periphery in two segments separated by tapering rifts which curve inward toward the nuclei.

[3] Occasionally, small dark markings, generally arcs or crescents, are found near the nuclei (e.g., N.G.C. 383, etc.), and in one case, M 87, exceedingly faint stars appear to crowd around the periphery.

having any given degree of flattening appear to exhibit the uniformity in luminosity distribution which is found among the lenticular images. So insignificant are the deviations from the standard forms that, were it not for the confusion introduced by the orientation, either the degree of flattening (the ratio of axes) or the luminosity gradient could be used indiscriminately to determine positions in the sequence.

The ideal classification should indicate the position of individual objects in the sequence of actual forms, independent of orientation. Theoretically this might be accomplished by a combination of the only two criteria available, the ellipticity of the projected images and the luminosity distribution. In practice, however, the application of the latter criterion to individual images is unsatisfactory. A round image may represent a nebula at any stage in the sequence, provided the minor axis is oriented in the line of sight, and the proper assignment by means of the luminosity distribution is still highly speculative. For this reason the images have been provisionally classified according to their ellipticities alone—criteria which are readily and rather accurately estimated from simple inspection of photographic plates and which furnish numerical symbols, on a decimal scale, so desirable in all classifications. This procedure presents the data ready for statistical discussion. Later, when the significance of the luminosity distribution is more fully established, symbols describing the luminosity gradients may be added as postscripts in order to complete the classification.

These considerations have led to the present investigations, which form a preliminary attempt to determine the actual luminosity distribution in the images of a selected list of elliptical nebulae. The results emphasize the homogeneity of elliptical nebulae as a group and suggest the dynamical pattern on which they are constructed.

The pioneer investigations along this line are due to J. H. Reynolds, who, in 1913,[1] found that the luminosity along the major axis of M 31, out to $7'$ from the nucleus, could be represented by the formula

$$\text{Luminosity} = \frac{\text{Constant}}{(x+1)^2},$$

[1] *Monthly Notices of the Royal Astronomical Society*, **74**, 132, 1913.

where x, the distance from the nucleus, was expressed in a unit equal to 34".5. The measures were restricted to the unresolved nuclear region and did not extend to the well-defined spiral arms. The result bears on the present investigations in view of the similarity between the nuclear regions of the earlier-type spirals and the later stages of the sequence of elliptical nebulae. Luminosity-curves derived at Mount Wilson for both classes of nebulae are expressed by the same type of formula as that found by Reynolds, although for M 31 the numerical values differ considerably from his.

In a second paper[1] Reynolds published curves for five other spirals representing wide variations in structure and resolution. With the scale employed the nuclear regions were rather small, however, and the results, which varied considerably from those for M 31, do not bear so directly on the problem of the elliptical nebulae.

METHOD OF INVESTIGATION

The procedure in the present investigation was as follows: For each nebula a series of exposures, usually from 15 minutes to 5 seconds, was made on a single Seed 30 or Eastman 40 plate at the Newtonian focus of the 100-inch reflector. Transparency-curves were then derived with the aid of a Koch registering microphotometer. For sensibly round images runs were made along one diameter only, but for elongated images, along both major and minor axes. Curves for the various images in a given series were then combined into single curves representing transparencies against distances from the nuclei. Finally, these curves were transformed into others representing luminosities as functions of nuclear distances.

The sensitive element in the microphotometer is a thermocouple constructed by Pettit.[2] Galvanometer deflections, strictly proportional to transparencies, were recorded as continuous curves on photographic plates geared to move at twenty times the speed with which the images moved across the aperture admitting the light-beam into the thermocouple. The aperture was square and of the order of 0.1 mm, or about 1".6, on a side. The range in galvanometer deflection, i.e., the deflection for the free film, was maintained at

[1] *Ibid.*, **80**, 746, 1920.

[2] *Journal of the Optical Society of America*, **7**, 137, 1923.

PLATE X

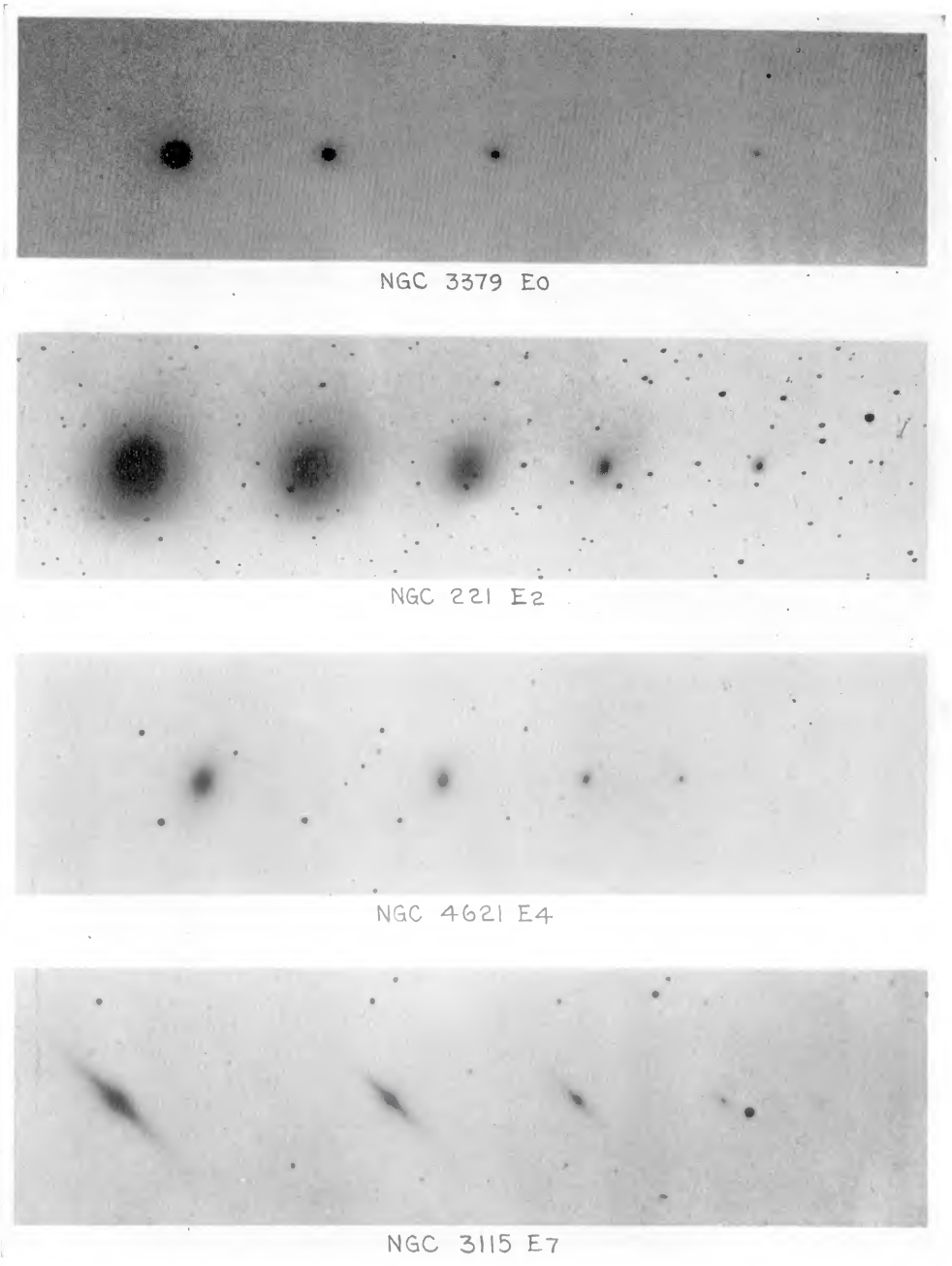

SUCCESSIVE EXPOSURES OF ELLIPTICAL NEBULAE PHOTOGRAPHED WITH THE 100-INCH REFLECTOR

about 4 inches. The linear scale of the recorded curves was, of course, twenty times the scale of the measured plates, or 1 mm = 0″.8.

MEASURES FOR N.G.C. 3379

The measures and reductions of N.G.C. 3379, an Eo nebula, furnish a typical example of the procedure. The series of images representing exposures of 15, 5, and 2 minutes, and 45 and 15 seconds, is illustrated in Plate X. Figure 1*a* shows the transparency-curves along diameters parallel with the equator, as photographically recorded by the Koch microphotometer. These were measured by laying the plate, film down, on accurately ruled co-ordinate paper, the intervals on which, 0.1 inch, furnished a convenient unit. In the horizontal direction this unit represented 2″.03 on the original negatives of the nebulae, while in the vertical direction the scale was arbitrary. Eventually, however, the vertical readings were transformed into decimals of the galvanometer deflection for the free film, in this case 36.2 units or 3.62 inches. The transparencies thus ranged from zero for complete blackening to 1.0 for the free film. Measures at the same distance on either side of the nuclei were combined, and in the outer regions of the images where the grain of the plate introduced irregularities some smoothing was necessary.

TABLE I

CORRECTIONS TO REDUCE *A* TO A LINEAR FUNCTION OF LOG *I*

TOE OF CURVE				SHOULDER OF CURVE	
A	Corr.	A	Corr.	A	Corr.
0.300	0.000	0.150	−0.077	0.760	0.000
.290	−0.002	.140	.087	.770	+0.001
.280	.004	.130	.098	.780	.003
.270	.007	.120	.111	.790	.007
.260	.010	.110	.127	.800	.011
.250	.013	.100	.146	.810	.016
.240	.017	.090	.168	.820	.021
.230	.021	.080	.193	.830	.026
.220	.026	.070	.222	.840	.032
.210	.031	.060	.254	.850	.039
.200	.037	.050	.290	.860	.048
.190	.043	.040	.331	.870	.057
.180	.050	.030	.382	.880	.067
.170	.058	0.020	−0.445	.890	.078
0.160	−0.067			0.900	+0.090

The measures are shown in Table II. In order to make larger readings correspond with greater luminosities in the nebula, the transparency-curves were inverted for measurement, and hence the tabulated values represent, not transparencies, but absorptions. By current definition, $A = 1 - T$. The problem of combining the absorption-curves for the various images of the series into a single curve representing the distribution of luminosity in the image with the longest exposure was solved in an empirical manner.

TABLE II

MEASURES OF N.G.C. 3379
(Values of 36.2—Galvanometer Deflection)*

r†	Exposure Time				
	15m	5m	2m	45s	15s
0	36.2	34.05	31.25	23.55	10.15
0.5	.....	33.75	30.7	21.5	8.7
1	35.8	33.3	28.4	17.85	5.9
1.5	.....	32.35	24.8	14.1	3.7
2	35.4	30.7	21.3	10.75	2.35
3	34.7	26.1	14.95	6.3	1.6
4	32.65	21.2	9.85	3.3	1.0
5	29.8	16.45	6.5	2.4	0.65
6	26.2	12.8	4.45	1.6	.4
7	22.75	9.4	3.15	1.1	.25
8	19.15	6.8	2.4	0.7	.1
9	16.25	5.3	1.6	.5	0.0
10	14.0	4.45	1.1	.3	
11	11.4	3.75	0.8	.2	
12	9.9	3.15	.6	.1	
13	8.9	2.8	.4	0.0	
14	7.45	2.4	.3		
15	6.8	2.15	.2		
16	5.9	1.85	.1		
17	5.45	1.65	0.0		
18	4.85	1.45			
19	4.25	1.25			
20	3.7	1.15			
22	2.8	0.8			
24	2.05	.6			
26	1.5	.3			
28	1.0	.1			
30	0.65	0.0			
32	.4				
34	.2				
36	.1				
38	0.0				

* Galvanometer deflection for free film = 3.62 in.
† Unit of r = 0.1 in. = 2".03.

CHARACTERISTIC ABSORPTION-CURVES

Characteristic absorption-curves for the type of plate employed were obtained in the laboratory. The time scales, $A = F(\log t)$, where the intensity is constant, and the intensity scales, $A = f(\log I)$, where t is constant, are of the general form shown in Figure 1. The linear portions of the time scales are parallel over a considerable range in I, and those of the intensity scale over a considerable range in t.

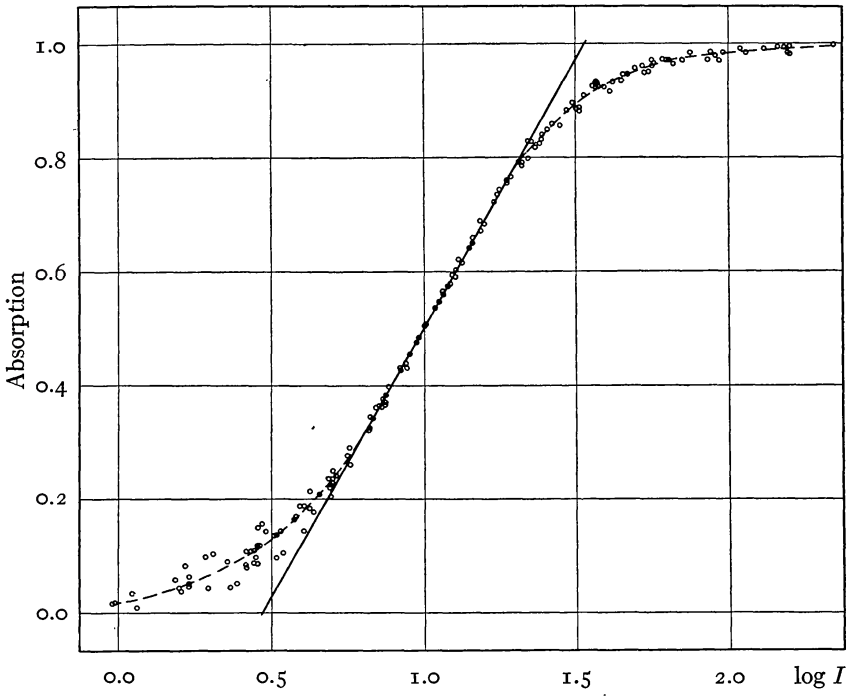

FIG. 1.—Characteristic absorption-curve for Eastman 40 plates exposed to sunlight

Especial attention was paid to the intensity scale since it affords the most direct method of converting a measured A into the corresponding luminosity. The curve in Figure 1 is a composite of twenty individual curves from Eastman 40 plates, exposed to sunlight through a varying-aperture densitometer and fully developed with a hydroquinone (X-ray) developer. Exposures ranged from 8 seconds to 30 minutes, and the transparencies of the films were varied by pre-exposures to simulate the sky fog on the nebular plates. The individual curves are all sensibly parallel, and were combined to form the composite curve by shifting along the axis of $\log I$.

The composite or standard intensity scale is approximately linear from $A=0.28$ to $A=0.78$, which covers 50 per cent of the range in galvanometer deflections. Corrections derived from the curve itself readily extend the usable linear relation over a range from $A=0.10$ to $A=0.90$. The table of corrections may be further extended, with diminishing accuracy, to the threshold of the plates; but in this region the measures themselves exhibit a considerable scatter, and consistency may be expected only in the general order of quantitative results. On the shoulder of the curve difficulties of another nature were encountered (Eberhard effect, etc.). These were not

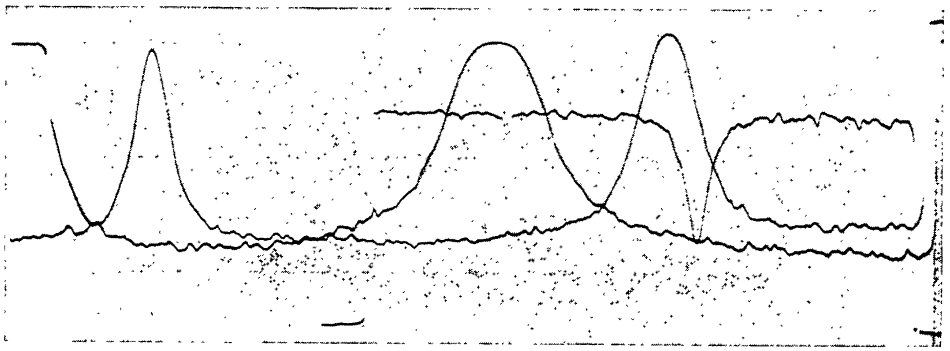

FIG. 1*a*.—Transparency-curves for images of N.G.C. 3379

fully investigated, but were avoided by using the shorter exposures for the bright nuclear regions of the nebulae.

The linear portion of the intensity scale is represented by the formula

$$\log I = 1.058A + \text{Constant}. \qquad (1)$$

The corrections used to extend this relation to the beginning of the shoulder and to the toe of the curve are given in Table I. These were derived from the composite curve, and were checked by comparing measured values of A at corresponding distances from the nuclei in the various images of a given nebula. The corrections are not of any high accuracy, but it is believed that they indicate the general order of the deviations down to about $A=0.02$.

The use of absorption-curves in the present investigations, rather than the conventional density-curves, requires explanation. The microphotometer measures transparencies in terms of galvanometer

deflections, hence the most convenient form of reduction-curve will be that which approximates a straight line over the largest and most reliable range in transparencies. These conditions appear to be met by a relation between intensities of the source and the deflections themselves, used either as transparencies, or, as in the procedure described above, as absorptions. The relation

$$\log I = f(A) \text{ or } f(T) ,$$

as shown in Figure 1, is approximately linear over the middle half of the range in deflections, $A = 0.28$ to $A = 0.78$, where the measures are most reliable. On the toe and the shoulder, which are rather symmetrical, the measures are less precise—on the shoulder, because the deflections themselves are relatively small; on the toe, because the grain of the plate becomes troublesome.

Near the threshold of the plates, corresponding to the toe of the absorption-curve, a linear reduction-curve may be obtained by plotting intensities directly against the deflections. In the form

$$I = f(A) \text{ or } f(T)$$

the data in Figure 1 give a sensibly linear relation from $A = 0.08$ to $A = 0.40$. This method straightens the toe of the absorption-curve at the expense of the shoulder.

The shoulder may be straightened at the expense of the toe by plotting the data in the form

$$\log I = f(\log A) \text{ or } f(\log T) .$$

Since density is defined as $-\log T$, this leads to the usual Hurter and Driffield curve, $\log I = f(D)$. In this form the data in Figure 1 give an approximately linear relation from $A = 0.68$ to $A = 0.98$. The linear range is only 60 per cent of that for the absorption-curve and, moreover, the accidental errors become increasingly troublesome in the upper regions where the galvanometer deflections are very small.

These three forms for the reduction-curve are adapted to different conditions, namely, moderate, low, and high densities, and hence offer a choice to fit particular requirements. For the present investigations, the first of these, $\log I = f(A)$, appears to be the best choice, not only for the reasons stated, but also because of definite incon-

veniences in the other forms. That for low densities, $I=f(A)$, introduces the question of units of luminosity, which is avoided by the use of log I. The density-curves, log $I=f(-\log T)$, appear to be more sensitive in the linear range to the Eberhard or some analogous effect. The latter possibility was tested by comparisons of the reduction-curve derived from a varying-aperture densitometer (Fig. 1) with those from photographic wedges with steep gradients. In the one case we are dealing with isolated patches within any one of which the photographic density is about constant; in the other, the density varies continuously across the negative. It is by no means certain that the development conditions for these two cases may be regarded as equivalent. The tests indicated that the absorption-curves, log $I=f(A)$, were similar over their linear ranges within the errors of observation, but that over the shoulders (the linear region of the density-curves) the curves from the wedges fell slightly but systematically below that from the densitometer. This discrepancy was not investigated further since the necessary reduction in the present study could be made without using the shoulders of the absorption-curves.

As a final test of the efficiency of the absorption-curves as a method of reduction, the wedges were replaced by positive copies from an original negative showing a series of images of a nebula. Transparency-curves of the positives were derived with the microphotometer. Second negatives were then made under the standard conditions, and measures of these negatives were compared with the transparencies of the positives.

Reduction-curves derived from these data agreed with those derived from the wedges, i.e., the absorption-curves agreed with those from the densitometer over the linear range, but over the shoulder they fell systematically below the densitometer-curves. Conversely, by using only the linear region of the reduction-curves previously derived, the transparency distribution in the positives could be reconstructed from the measures of the second negatives with a fair degree of accuracy—say 2 per cent of the central transparency. This last test encourages the belief that the present investigations lead to a fairly reliable representation of luminosity distribution in the images of elliptical nebulae.

REDUCTION OF MEASURES FOR N.G.C. 3379

We may now return to the measures of N.G.C. 3379. The corrections in Table I reduced the values of A for the curves of the various nebular images to quantities proportional to log I over a considerable range in the measured A. The corrected curves were

TABLE III

REDUCTION OF MEASURES OF N.G.C. 3379

r	15m		5m		2m		45s		15s	Combined	
	A	ΔA	A	ΔA	A	ΔA	A	ΔA	A	A	log I
0	.....	.....	.....	.....	0.914	.....	+0.651	0.375	+0.276	+1.634	+1.729
0.5	.....	.....	.....	.....	.886	0.292	.594	.371	.223	1.588	1.680
1	.....	.....	.....	.....	.788	.295	.493	.393	+ .100	1.480	1.566
1.5	.....	.....	.....	.....	.685	.296	.389	0.429	−0.040	1.375	1.451
2	.....	.....	+0.886	0.298	.588	.291	.297	.....	.....	1.274	1.348
3	.....	.....	.721	.308	.413	0.293	+ .120	.....	.....	1.102	1.166
4	.....	.....	.586	.322	.264	.....	−0.057	.....	.....	0.958	1.014
5	+0.846	+0.392	.454	.323	.131	.....	.....	.....	.....	.833	0.881
6	.724	.370	.354	0.335	0.019	.....	.....	.....	.....	.721	.763
7	.628	.378	.250	.....	.....	.....	.....	.....	.....	.627	.663
8	.529	.385	.144	.....	.....	.....	.....	.....	.....	.524	.554
9	.449	.383	.066	.....	.....	.....	.....	.....	.....	.445	.471
10	.387	.370	+ .017	.....	.....	.....	.....	.....	.....	.390	.413
11	.315	0.349	−0.034	.....	.....	.....	.....	.....	.....	.328	.347
12	.267	.....	.....	.....	.....	.....	.....	.....	.....	.267	.282
13	.227	.....	.....	.....	.....	.....	.....	.....	.....	.227	.240
14	.172	.....	.....	.....	.....	.....	.....	.....	.....	.172	.182
15	.144	.....	.....	.....	.....	.....	.....	.....	.....	.144	.152
16	.100	.....	.....	.....	.....	.....	.....	.....	.....	.100	.106
17	.076	.....	.....	.....	.....	.....	.....	.....	.....	.076	.080
18	.042	.....	.....	.....	.....	.....	.....	.....	.....	.042	.044
19	+ .001	.....	.....	.....	.....	.....	.....	.....	.....	+ .001	+ .001
20	− .040	.....	.....	.....	.....	.....	.....	.....	.....	− .040	− .042
22	− .127	.....	.....	.....	.....	.....	.....	.....	.....	− .127	− .134
24	− .213	.....	.....	.....	.....	.....	.....	.....	.....	− .213	− .225
26	− .286	.....	.....	.....	.....	.....	.....	.....	.....	− .286	− .303
28	− .366	.....	.....	.....	.....	.....	.....	.....	.....	− .366	− .387
30	−0.447	.....	.....	.....	.....	.....	.....	.....	.....	−0.447	−0.473

	ΔA		ΔA
15m − 5m	0.375	15m − 5m	0.375
5 − 2	.317	15 − 2	.692
2 −45s	.293	15 −45s	.985
45s −15	0.398	15 −15	1.383

approximately parallel, as was to be expected, since time scales are parallel over a wide range in log I, and were brought into coincidence by displacement along the axis of A by amounts representing the differences in exposure time. The displacements were determined from the overlap of the curves themselves (in practice between corrected $A = 0.0$ to $A = 0.80$), and the entire series was combined into a single absorption-curve representing the image of longest exposure. The reduction for N.G.C. 3379 is shown in Table III.

The relation between displacements, ΔA, and relative exposures, $\log t_0/t$, where t_0 is the longest exposure, furnish a check against the time scale. For N.G.C. 3379 the data in Table III indicate the relation $\Delta A = 0.78 \log t_0/t$. Remeasurement of this plate gave the coefficient 0.785. The average for all the plates of the observed nebulae is about 0.80, which agrees with the slope of the time scales obtained in the laboratory.

LUMINOSITY-CURVE FOR N.G.C. 3379

The final step in the reduction of the measures of N.G.C. 3379 was the conversion of the combined values of A into $\log I$ by means of formula (1). This gave the relation between luminosity, I, and distance from the nucleus, r, which is shown graphically in Figure 2, in three different forms. The curve to the left, 2*a*, represents $\log I = f(r)$. Curve 2*b* corresponds to $\log I = f(\log r)$. A simple inspection indicates that the second curve may be transformed into an approximately linear relation by adding a constant to the successive values of r. The necessary constant was found by trial to be 2.4, which is equivalent to $4''.9$, and the slope of the straight line thus obtained was so close to 2.0 that the exact integer was accepted and the line so drawn with a straight edge through the points in 2*c*. The relation

$$\log I = 2.62 - 2 \log (r + 2.4)$$

fits the data from near the nucleus to distances at which the luminosities are far down on the toe of the intensity scale, with an accuracy within the probable errors of the observations.

A second set of microphotometer curves from the same negative gave

$$\log I = 2.64 - 2 \log (r + 2.3) .$$

The means of the two sets of measures gave the adopted equation

$$\log I = 2.62 - 2 \log (r + 2.3) .$$

The values of $\log I$ from the two sets of measures show a systematic difference of 0.016 between $\log I = 1.7$ and -0.1, and an average residual of ± 0.018.

INDIVIDUAL LUMINOSITY-CURVES FOR FIFTEEN ELLIPTICAL NEBULAE

The results for N.G.C. 3379 are typical of those found for elliptical nebulae in general, fifteen of which (Table IV) were investigated

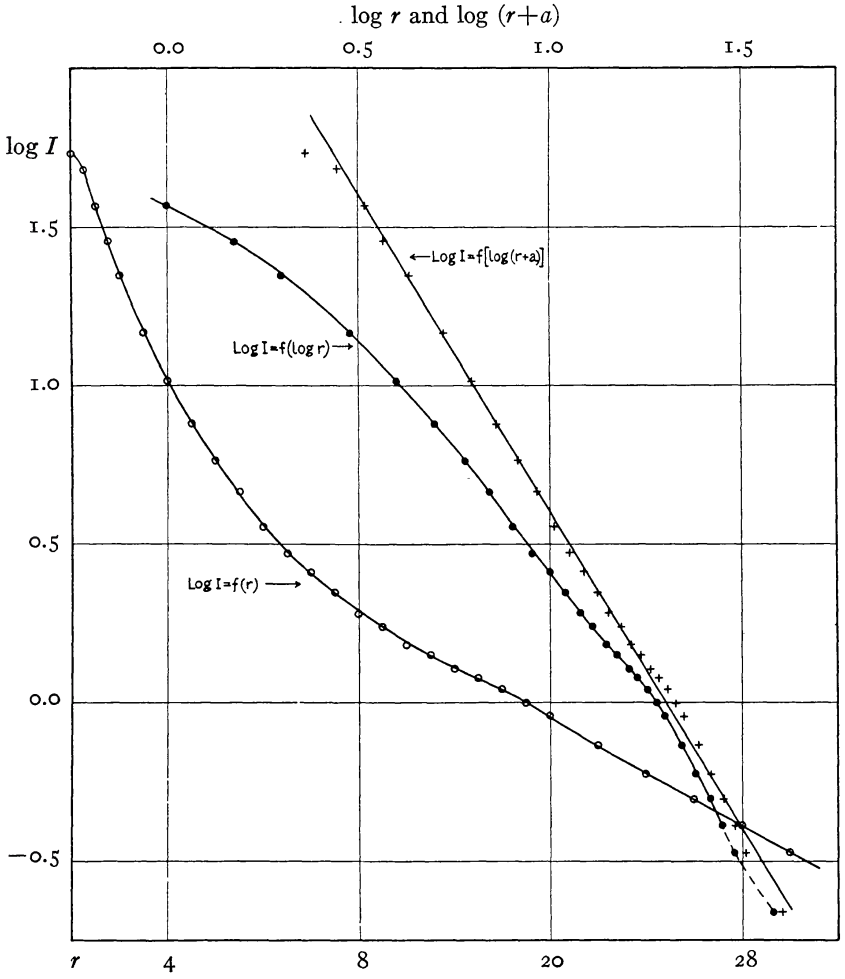

FIG. 2.—Luminosity-curve for the image of N.G.C. 3379

along various diameters, and for the unresolved nuclear regions of at least some of the earlier-type spirals.

The curves were constructed as described for N.G.C. 3379. The four nebulae with sensibly round images, N.G.C. 3379, 4283, 4486, and 4552, were measured along a single diameter, usually that parallel to the equator. For N.G.C. 584, also measured but once, the particular diameter is indicated.

In each object the distribution of luminosity may be represented by a formula of the type

$$\log I = K - 2 \log (r+a) , \tag{2}$$

where a varies from nebula to nebula and, in any elongated nebula, with the diameter along which the luminosities were measured.

Let I_0 be the central luminosity; then $K = \log I_0 a^2$ and formula (2) may be written

$$\log I = \log I_0 - 2 \log \left(\frac{r}{a}+1\right) , \tag{3}$$

or

$$I = \frac{I_0}{\left(\frac{r}{a}+1\right)^2} . \tag{4}$$

Formula (3) permits a direct comparison of luminosity-curves along various diameters of different nebulae. If $\log I$ is expressed as a function of r/a instead of simply a, the curves are all parallel and are displaced along the axis of $\log I$ by amounts corresponding to differences in $\log I_0$. The curves can then be shifted into coincidence, giving a mean curve for all the nebulae observed, reduced to a standard $\log I_0$.

The constants of the empirical formulae representing the various luminosity-curves, namely, K, a, and $\log I_0$, are listed in Table IV. The third column gives the exposure time of the strongest image in the series measured. The fifth column indicates the quality of the results as judged from the appearance of the plates and the irregularities and discrepancies in the curves for different images in the same series. The other data are self-explanatory.

The actual measures for each nebula are not tabulated, but Table V gives the values of $\log I$ for successive values of r/a, reduced to $\log I_0 = 2.0$ as a standard. These were obtained by adding to each value of $\log I$ measured on any curve the quantity $2.0 - \log I_0$, where I_0 has the value listed in Table IV. These corrections merely shift the curves parallel to themselves along the axis of $\log I$. By reversing the operation the original curves may be derived from Table V, and with the values of a given in Table IV, the measures themselves may be read from the curves for successive values of r.

ACCURACY OF THE MEASURES

Luminosities on the toe of the intensity scale below log $I=0.0$ become increasingly uncertain, but are included in the hope that mean values for several curves may have some significance. Reference to the standard intensity scale in Figure 1 emphasizes the large scatter among the measures in this region and the consequent

TABLE IV

PARAMETERS FOR LUMINOSITY-CURVES OF INDIVIDUAL NEBULAE

N.G.C.	Type	Exp.	Diam.	Q	a	K	log I_o
221*	E2	22^m	Min.	G	2.5	3.14	2.344
			Maj.	G	3.1	3.342	2.359
410	E2	60	Min.	G	2.0	2.30	1.698
			Maj.	G	2.6	2.54	1.710
584	E4	20	30°†	P	1.7	2.205	1.744
3115*	E7	15	Min.	G	1.4	2.21	1.918
			Maj.	G	5.0	3.15	1.752
3379*	E0	15	.....	G	2.3	2.62	1.897
4278*	E1	15	Min.	G	1.2	2.04	1.880
			Maj.	F	1.8	2.20	1.689
4283	E0	15	.....	G	1.0	1.60	1.600
4374	E1	15	Min.	F	2.2	2.33	1.645
			Maj.	P	3 0	2.55	1.596
4382	E4	15	Min.	P	2.0	2.35	1.748
			Maj.	P	3.6	2.72	1.607
4406*	E2	15	Min.	F	2.4	2.40	1.640
			Maj.	F	3.2	2.60	1.590
4472*	E1	15	Min.	G	3.3	2.74	1.703
			Maj.	G	4.5	2.90	1.594
4486	E0	15	.....	F	4.6	2.66	1.334
4552	E0	15	.....	G	1.9	2.40	1.842
4621	E5	15	Min.	F	1.5	2.25	1.873
			Maj.	F	2.8	2.67	1.776
4649*	E2	15	Min.	G	2.6	2.57	1.740
			Maj.	G	3.6	2.75	1.638

* Mean of two or more plates.

† Inclination of measured diameter to major axis.

uncertainty in the exact delineation of the curve as it approaches the threshold of the plate almost asymptotically to the axis of log I. Very slight errors in the delineation are greatly magnified in the table of corrections which convert the measured values of A into a linear function of log I. Relatively large errors, both systematic and accidental, therefore probably occur among the low values of log I in Table V.

Very high values of log I are subject to uncertainties arising from

the combination of several curves from successively weaker images into a single mean curve. Values of a are sensitive to errors in the upper region of the composite curves. The order of the errors involved may be estimated from remeasures made on eight of the original plates. Systematic differences in log I for log $I > -0.100$ ranged from 0.016 to 0.035, with a mean of 0.025, or 2.5 per cent of the galvanometer deflection for the free film. Average residuals ranged from 0.007 to 0.018.

Measures from duplicate negatives of the same object were made for seven nebulae. Here the systematic differences in log I were much larger, owing to differences in the transparency of the sky, in the silver coats on the mirrors of the telescope, and possibly in the sensitivity of the plates. The maximum systematic difference in log I was 0.160 for two 15-minute exposures of N.G.C. 4472. Average residuals above log $I = -0.100$, however, were only 0.010 and 0.020 for the minor and major diameters, respectively. With one exception the average residuals for all the nebulae lie between 0.012 and 0.025.

TABLE V

LUMINOSITY-CURVES REDUCED TO STANDARD LOG I_0

N.G.C.	r/a									
	0.0	0.25	0.5	0.75	1.0	1.5	2.0	2.5	3.0	3.5
221 min	1.969	1.846	1.631	1.521	1.381	1.176	1.021	0.896	0.791	0.711
maj	1.911	1.841	1.646	1.521	1.416	1.221	1.066	.941	.831	.731
410 min	1.895	1.812	1.672	1.522	1.382	1.182	1.042	.912	.802	.692
maj	1.909	1.835	1.680	1.510	1.390	1.170	1.030	.900	.800	.700
584	1.794	1.736	1.636	1.496	1.401	1.216	1.066	.946	.846	.736
3115 min	1.700	1.672	1.612	1.532	1.432	1.222	1.072	.937	.827	.707
maj	1.977	1.823	1.628	1.478	1.373	1.208	1.048	.918	.798	.703
3379	1.845	1.793	1.658	1.543	1.408	1.213	1.053	.893	.778	.663
4278 min	1.720	1.690	1.620	1.502	1.382	1.197	1.047	.917	.807	.692
maj	1.833	1.792	1.662	1.512	1.387	1.192	1.042	.912	.792	.682
4283	1.574	1.560	1.525	1.460	1.380	1.215	1.070	.950	.825	.720
4374 min	1.836	1.785	1.655	1.505	1.400	1.185	1.025	.900	.795	.710
maj	1.799	1.764	1.644	1.519	1.394	1.184	1.034	.904	.789	.694
4382 min	1.862	1.802	1.692	1.542	1.412	1.202	1.022	.892	.797	.712
maj	1.963	1.868	1.663	1.503	1.378	1.153	0.973	.838	.743	.663
4406 min	1.954	1.860	1.660	1.490	1.360	1.150	0.990	.880	.770	.680
maj	1.963	1.835	1.635	1.470	1.350	1.160	1.010	.890	.785	.695
4472 min	1.847	1.777	1.647	1.522	1.377	1.177	1.012	.882	.787	.692
maj	1.940	1.856	1.676	1.506	1.391	1.181	1.036	.911	.806	.746
4486	1.851	1.771	1.651	1.541	1.441	1.236	1.076	.936	.816	.701
4552	1.761	1.738	1.648	1.508	1.408	1.228	1.063	.903	.783	.683
4621 min	1.834	1.797	1.657	1.517	1.392	1.192	1.037	.897	.787	.692
maj	1.908	1.844	1.684	1.529	1.414	1.194	0.999	.869	.764	.674
4649 min	1.781	1.760	1.650	1.550	1.445	1.240	1.070	.930	.810	.700
maj	1.820	1.772	1.667	1.532	1.412	1.202	1.042	0.912	0.782	0.682

TABLE V—*Continued*

N.G.C.	r/a									
	4.0	4.5	5	6	7	8	9	10	12	14
221 min	0.626	0.546	0.481	0.351	0.226	+0.111	+0.006	−0.094	−0.264	−0.474
maj	.636	.556	.476	.326	.191	.091	− .009	− .099	− .234	− .354*
410 min	.597	.517	.437	.287	.162	.052	− .078	− .170	.....	.....
maj	.610	.545	.480	.350	.230	+ .110	+ .030	− .130	.....	.....
584	.636	.546	.456	.281	.116	− .004	− .084	− .144	− .244	.....
3115 min	.622	.542	.457	.312	.192	+ .097	+ .012	− .078	− .218	− .338†
maj	.613	.528	.453	.328	.178	.013	− .122	− .277	.....	.....
3379	.578	.503	.428	.308	.208	.123	+ .023	− .067	− .243	− .412
4278 min	.597	.502	.412	.267	.152	.047	− .043	− .108	− .168	− .318
maj	.572	.482	.397	.232	.102	.022	− .058	− .108	− .208	− .288
4283	.610	.505	.420	.225	.165	.085	+ .015	− .050	− .120	− .150
4374 min	.625	.550	.480	.355	.245	.095	− .035	− .135	.....	.....
maj	.624	.564	.509	.394	.279	.184	+ .104	+ .004	.....	.....
4382 min	.647	.582	.522	.412	.307	.202	+ .112	+ .027	− .153	− .323
maj	.593	.528	.478	.383	.308	.223	+ .143	+ .043	− .107	.....
4406 min	.595	.525	.465	.340	.235	.135	+ .050	− .030	− .205	.....
maj	.615	.540	.480	.365	.265	.120	+ .060	− .060	.....	.....
4472 min	.602	.522	.452	.342	.247	.157	+ .067	− .013	− .203	.....
maj	.636	.566	.491	.371	.276	+ .194	+ .111	+ .046	− .139	.....
4486	.591	.486	.376	.195	.076	− .014	.....	.....	.....	.....
4552	.598	.523	.443	.313	.208	+ .108	+ .003	− .107	− .317	.....
4621 min	.612	.532	.467	.327	.212	.112	− .003	− .123	− .333	− .453
maj	.604	.534	.469	.344	.224	.114	− .001	− .104	− .286	− .446
4649 min	.610	.530	.450	.320	.170	.065	− 0.50	− .150	− .370	.....
maj	0.592	0.522	0.457	0.337	0.227	+0.122	+0.032	−0.063	−0.218	−0.328

* Values for $r/a = 16$, 18, and 20 are 0.464, 0.639, and 0.824, respectively.
† Values for $r/a = 16$, 18, and 20 are 0.418, 0.513, and 0.588, respectively.

The exception is N.G.C. 3115, for which the curve along the minor axis derived from the two plates gave perceptibly different slopes, amounting to 0.160 in log I at $r = 19$. The source of this discrepancy was traced to imperfections in the film, affecting two images, on one of the plates. The series of measures thus affected was discarded.

The values of a derived from the seven duplicate plates afforded ten comparisons. The differences averaged about 5 per cent and in no case exceeded 10 per cent. This was rather unexpected, for the determinations of a were made by trial and error and involved a certain amount of compromise and adjustment. In certain cases slightly modified values of a combined with coefficients of log $(r/a+1)$, differing a little from 2.0, would fit the data as well or possibly better than the adopted values. Since the possible deviations in the coefficient are small and the values clustered closely around 2.0, the exact integer was used in each case and the value of a adjusted to fit. The justification for this rather arbitrary procedure lies in the fact that the deviations are within the range of observational errors and of

the differences between the means of the values in Table V with those computed from formula (3).

MEAN LUMINOSITY-CURVE FOR ELLIPTICAL NEBULAE IN GENERAL

The comparison of the mean luminosity-curve based on the individual curves in Table V with that defined by the standard relation

$$\log I = 2 - 2 \log (r/a + 1)$$

is tabulated in Table VI and is shown graphically in Figure 3.

TABLE VI

MEAN LUMINOSITY-CURVE FOR PROJECTED IMAGES OF ELLIPTICAL NEBULAE

r/a	log I			No.
	Cal.	Obs.	C−O	
0	+2.000	+1.853	+0.147	25
0.25	1.806	1.780	+ .026	25
0.5	1.648	1.647	+ .001	25
0.75	1.514	1.509	+ .005	25
1	1.398	1.396	+ .002	25
1.5	1.204	1.196	+ .008	25
2	1.046	1.039	+ .007	25
2.5	0.912	0.907	+ .005	25
3	.796	.797	− .001	25
3.5	.694	.702	− .008	25
4	.602	.610	− .008	25
4.5	.519	.531	− .012	25
5	.444	.458	− .014	25
6	.310	.322	− .012	25
7	.194	.208	− .014	25
8	+ .092	.104	− .012	25
9	.000	+ .012	− .012	24
10	− .083	− .083	.000	24
12	− .228	− .238	+ .010	18
14	− .352	− .353	+ .001	11
16	− .461	− .441	− .020	2
18	− .558	− .576	+ 018	2
20	−0.644	−0.706	+0.062	2

The large C−O for $r/a = 0.0$ is at least partially explained by the method of measurement. The observed log I_0 represents the average luminosity over the area covered by the slit in the microphotometer, while the calculated value refers to a central point from which the luminosity is assumed to fall rapidly in all directions. The observed

values are thus necessarily smaller than the calculated. Since the area of the slit remains constant, the effect increases with the luminosity gradient, or as a decreases. This is shown graphically in Figure 4 as a relation between a and the observed log I_0 given in Table V. The point $r/a=0.25$ is similarly affected, although to a less de-

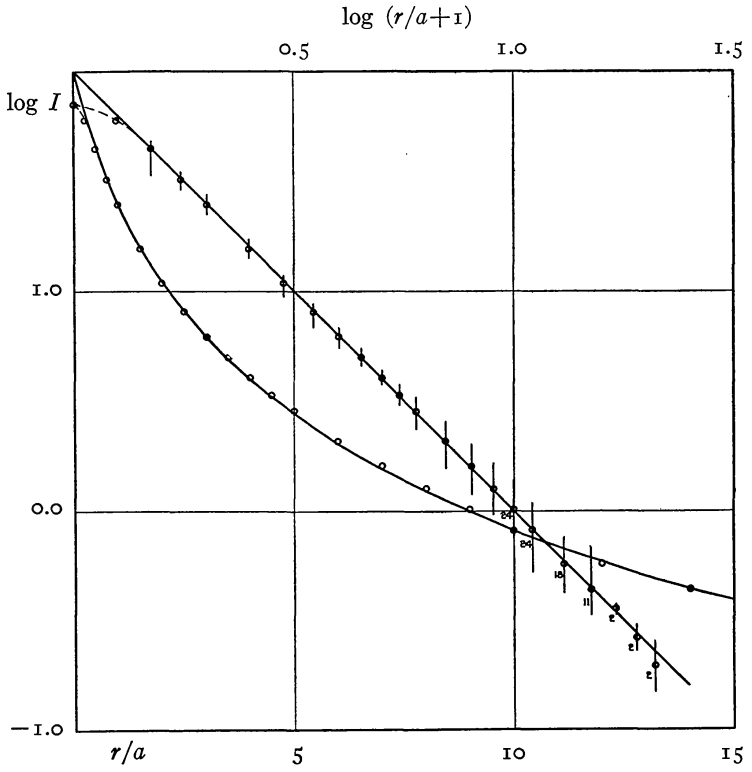

FIG. 3.—Combined luminosity-curve for the images of elliptical nebulae. The vertical lines represent the scatter among the individual curves. The figures indicate the number of individual curves included in the mean. Above log $I=0.0$ the number for each point is 25.

gree. The influence is especially noticeable where a is small. For N.G.C. 3115 min. ($a=1.4$), 4278 min. ($a=1.2$), and 4283 ($a=1.0$), the values of C−O for $r/a=+0.25$ are +0.134, +0.116, and +0.246, respectively. The rejection of these three residuals reduces the mean C−O for this point from 0.026 to 0.007. The remainder of the data to $r/a=14$, beyond which the number of curves is too small for precision, shows an average C−O of about 0.0075. The dispersion

in log I is of the order of 0.100 out to $r/a = 5.0$, beyond which the scatter increases, owing probably to the uncertainties in the low values of log I for the fainter nebulae.

The relatively small dispersion in the composite curve suggests that the empirical formula (3) holds out to the limit of measurement. The data for the outer regions are weak, however, even for the brighter nebulae, and must be accepted with caution. Further information on the outer regions has been sought in supplementary measures of such long exposures as were available, and in the correla-

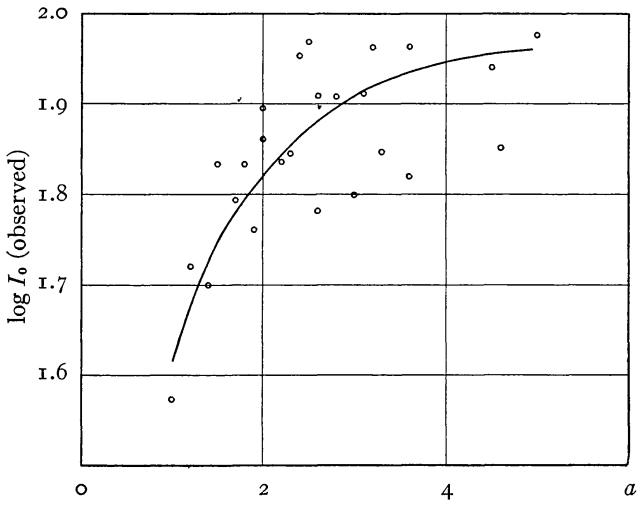

FIG. 4.—Relation between the observed central luminosity and the parameter a

tion of diameters, as measured with the microphotometer, with central luminosities and with exposure times.

SUPPLEMENTARY MEASURES ON LONG EXPOSURES

Exposures ranging from one to two hours on Eastman 40 plates developed with X-ray developer were available for seven of the nebulae given in Table IV. Absorption-curves of these images were recorded, measured, and reduced in the manner previously described, and were combined with the earlier results to obtain luminosity-curves running from the nuclei out to the thresholds of the long exposures. The combined results are given in Table VII with the values of log I for successive values of r/a reduced to a standard log $I_0 = 2.0$.

TABLE VII

LUMINOSITY-CURVES FROM LONG EXPOSURES, REDUCED TO STANDARD LOG I_0

r/a	221		4278		4283	4406	
	Min.	Maj.	Min.	Maj.		Min.	Maj.
4*.....	+0.626	+0.636	+0.613	+0.602	+0.612	+0.598	+0.620
5.....	.481	.476	.448	.425	.430	.462	.508
6.....	.357	.326	.273	.275	.286	.345	.410
8.....	+ .113	+ .095	+ .058	+ .070	+ .090	+ .150	.220
10.....	− .090	− .103	− .082	− .058	− .070	− .010	+ .080
12.....	.267	.275	.212	.172	.185	.160	− .045
14.....	.420	.450	.312	.290	.317	(.260)	.145
16.....	.550	.560	.392	.380	(.386)	(.360)	(.230)
18.....	.680	.675	.477	.475	(.473)	(.455)	(.355)
20.....	.790	.780	.564	(.576)	(.542)	(−0.525)	(−0.470)
22.....	0.905	.845	.662	(.670)	(.589)	.....	.....
24.....	(1.000)	0.920	.762	(.765)	(−0.652)	.....	.....
26.....	(1.100)	(1.000)	(.842)	(−0.905)	.....	.....	.....
28.....	(1.190)	(1.050)	(0.912)	.....	.....	.....	.....
30.....	(−1.280)	(1.150)	(1.012)	.....	.....	.....	.....
32.....	.....	(−1.250)	(−1.098)	.....	.....	.....	.....
	−0.800	−0.800	−0.560	−0.360	−0.170	−0.020	+0.020

r/a	4472		4486	4621		Mean	
	Min.	Maj.		Min.	Maj.	Obs.	Cal.
4*.....	+0.596	+0.636	+0.570	+0.595	+0.610	+0.609	+0.602
5.....	.451	.500	.405	.445	.470	.458	.444
6.....	.346	.400	.270	.300	.355	.331	.310
8.....	.171	.255	+ .075	+ .135	.165	+ .133	+ .092
10.....	+ .040	.120	− .080	− .022	+ .030	− .020	− .083
12.....	− .045	+ .010	.210	.130	− .090	.148	.228
14.....	.135	− .115	.320	.225	.210	.267	.352
16.....	.235	.260	.420	.320	.315	.367	.461
18.....	.335	(.405)	.525	.410	.430	.475	.558
20.....	(.435)	(.560)	.640	.490	(.550)	.577	.644
22.....	(.550)	(−0.685)	(.795)	.545	(.650)	.684	.723
24.....	(−0.670)	.....	(0.900)	.620	(−0.760)	.783	.796
26.....	.....	.....	(−1.030)	(.685)	.....	.927	.863
28.....	.....	.....	.....	(.745)	.....	0.974	.925
30.....	.....	.....	.....	(.820)	.....	1.065	0.983
32.....	.....	.....	.....	(−0.880)	.....	−1.076	−1.037
	−0.340	−0.210	−0.530	−0.420	−0.280	.....	.....

* Log I for $r/a<4$ may be found in Table V. The quantities at the bottom of each column are the corrections applied to the measured values of log I in order to reduce them to the standard log $I_0=2.0$. Values inclosed in parentheses are from the toe of the characteristic intensity scale (log $I<-0.2$) and are uncertain.

These data were not incorporated in the preceding discussion because the long exposures were not made with this particular end in view and the standard conditions may not always have been strictly maintained. Moreover, the photometric properties of long exposures were not investigated in the laboratory, but were assumed to approximate extrapolations of the relations among the shorter ex-

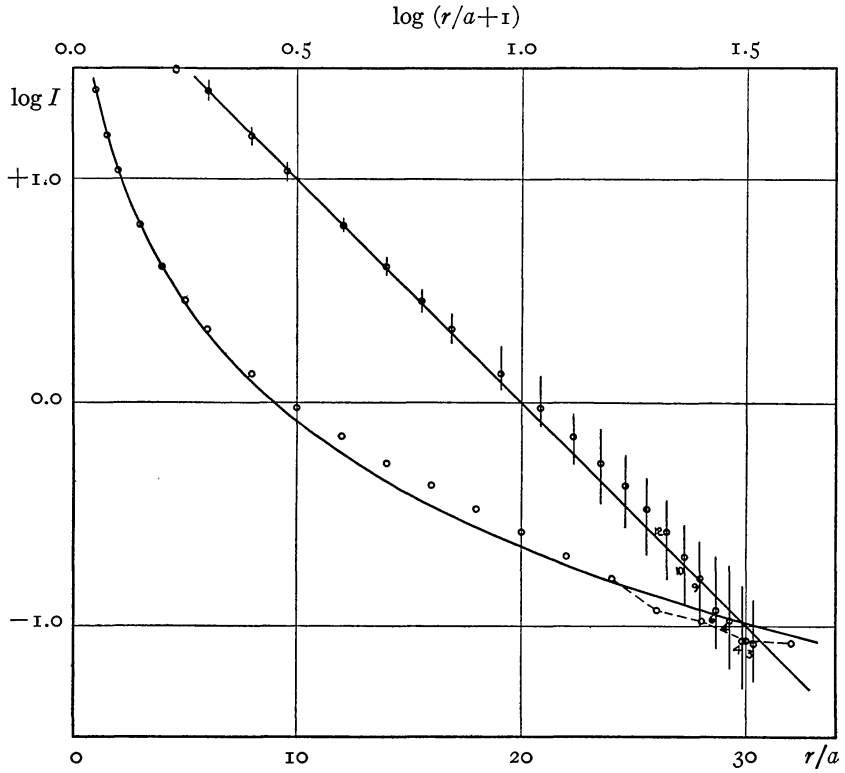

FIG. 5.—Combined luminosity-curve for images of elliptical nebulae derived from long exposures. The vertical lines represent the scatter among the individual curves. The figures indicate the number of individual curves included in the mean. Above log $I = -0.5$ the number for each point is 12.

posures. It was possible, however, to check the time scale from the data themselves, as will be shown in a later paragraph, and this substantially supports the reliability of the results.

In Figure 5, where the means of log I have been plotted against r/a, the data follow the general course of the formula out to points near the limits of the measures. The slight deviations between $r/a = 10$ and 20 appear to be real and may be significant in view of the

purely empirical nature of the formula. Deviations in the opposite direction beyond $r/a = 30$ depend upon a very few uncertain values and probably have less significance.

RELATION BETWEEN DIAMETER AND CENTRAL LUMINOSITY

A second method of testing formula (3) in the outer regions of low luminosity consists in comparing measured diameters of images with diameters computed from $\log I_0$ and the constant threshold value of $\log I$. Diameters measured from the microphotometer curves are rather uncertain, owing to irregularities in the grain of the plates and the almost asymptotic slope of the curve near the threshold; but the errors are largely accidental and may be reduced by multiplying the observations. The value of $\log I$ at the threshold is also uncertain, but in the discussion which follows, this enters as a constant to be determined on the assumption that it does not vary systematically with the exposure time. This assumption may be questionable, but at least it will serve as a first approximation.

If formula (3) holds beyond the limits of the measures, then, at the threshold of a plate,

$$\log I_0 = 2 \log R + \log I_{Th} , \tag{5}$$

where $R = r'/a + 1$, in which r'/a is the semidiameter in units of a, and $\log I_{Th}$ is the threshold value of $\log I$. Relation (5) may be tested by plotting $\log I_0$ against $\log R$ for all the images available.

The observational data are collected in Table VIII. The first group comprises twelve nebulae (twenty luminosity-curves), for which the exposures of the images measured range from 15 minutes to 45 seconds, with additional 15-second exposures for two of the nebulae (four curves), and additional long exposures for six of the nebulae (ten curves). These are followed by data for N.G.C. 410 and 584, and finally in Table VIII*a* for N.G.C. 221, with exposure times differing not only from those of the first group but also among themselves. The significance of the exposure times, which are irrelevant to the testing of formula (5), will be indicated later.

The plot of $\log I_0$ against $\log R$ is shown in Figure 6. The straight line is the relation

$$\log I_0 = 2 \log R - 0.740 , \tag{6}$$

TABLE VIII

SEMIDIAMETERS AND CENTRAL LUMINOSITIES FOR VARIOUS EXPOSURE TIMES

N.G.C.	0.25m		0.75m		2m		5m		15m		Long Exposures		
	log R	log I_o	log R	log I_o	log R	log I_o	log R	log I_o	log R	log I_o	log R	log I_o	log Exp.
3115* min	0.803	0.506	0.911	0.934	1.013	1.220	1.130	1.521	1.307	1.918	.....	.....	.....
maj	.491	.262	.663	.660	0.839	1.008	0.968	1.360	1.100	1.752	.....	.....	.....
3379*	.....	.....	.744	.860	0.934	1.157	1.127	1.489	1.255	1.897	.....	.....	.....
4278* min	.....	.....	.869	.747	1.004	1.097	1.072	1.483	1.283	1.880	1.574	2.560	1.778
maj	.....	.....	.778	.595	0.869	0.927	1.065	1.259	1.220	1.689	1.505	2.360	1.778
4283*	.....	.....	.699	.487	.903	.837	1.114	1.211	1.255	1.600	1.491	2.170	1.778
4374 min	.....	.....	.707	.578	.893	.969	1.004	1.280	1.137	1.645	.....	.....	.....
maj	.....	.....	.727	.563	.865	0.894	1.041	1.217	1.136	1.596	.....	.....	.....
4382 min	.....	.....	.845	.719	.978	1.037	1.114	1.373	1.230	1.748	.....	.....	.....
maj	.....	.....	.637	.558	.817	0.908	0.970	1.210	1.173	1.607	.....	.....	.....
4406* min	.....	.....	.633	.461	.806	.852	.989	1.192	1.196	1.640	1.385	2.020	1.903
maj	.....	.....	.580	.436	.740	.800	0.914	1.154	1.140	1.590	1.405	1 980	1 903
4472* min	.....	.....	.636	.506	.810	.887	1.004	1.258	1.208	1.703	1.447	2.340	2.079
maj	.....	.....	.614	.407	.838	.784	0.954	1.138	1.170	1.594	1 406	2.210	2.079
4486	.....	.....	.478	.400	.691	0.628	.794	0.777	0.987	1.334	1.497	2.530	2.079
4552	.....	.....	.691	.606	.823	1.008	0.946	1.346	1.090	1.742	.....	.....	.....
4621 min	.565	.318	.699	.683	.885	1.093	1.114	1.474	1.230	1.873	1.602	2.420	1.778
maj	0.497	0.173	.624	.570	.751	0.951	0.964	1.312	1.204	1.776	1.438	2.280	1.778
4649* min	.....	.....	.686	.597	.831	.956	.939	1.322	1.149	1.740	.....	.....	.....
maj	.....	.....	0.648	0.566	0.778	0.903	0.854	1.215	1.164	1.638	.....	.....	.....
Mean	(0.589)	(0.320)	.....	.....	.....	.....	.....	.....	.....	.....	(1.475)	(2.287)	.....
	0.524	0.189	0.693	0.597	0.853	0.946	1.004	1.279	1.182	1.698	1.468	2.317	1.893

N.G.C.	0.63m		1.25m		2.5m		5m		10m		20m		
584	0.757	0.590	0.873	0.787	0.873	1.122	0.906	1.403	0.993	1.547	1.144	1.744	
	0.7m		2.2m		6.7m		20m		60m				
410 min	.....	.....	0.544	0.430	0.653	0.819	0.903	1.193	1.114	1.698			
maj	0.405	−0.021	0.567	0.377	0.686	0.805	0.877	1.265	1.098	1.710			

which fits the lower end of the plot where formula (3) is known to hold. The constant, −0.740, represents the threshold value of log I and is of the same general order as that estimated from the extra-

TABLE VIII*a*

N.G.C. 221*

Exp.	Min.		Maj.		Mean	
	log R	log I_0	log R	log I_0	log R	log I_0
8^m.....	1.532	2.800	1.602	2.800	1.567	2.800
22.....	1.326	2.344	1.342	2.359	1.334	2.351
11.....	1.260	2.057	1.281	2.144	1.270	2.100
4.5.....	1.176	1.716	1.163	1.819	1.170	1.768
1.83.....	1.057	1.349	1.015	1.407	1.036	1.380
0.5.....	0.823	0.965	0.852	1.001	0.837	0.983
0.15.....	0.602	0.474	0.591	0.512	0.597	0.493

* Mean of two or more plates (asterisk has same meaning in Table VIII).

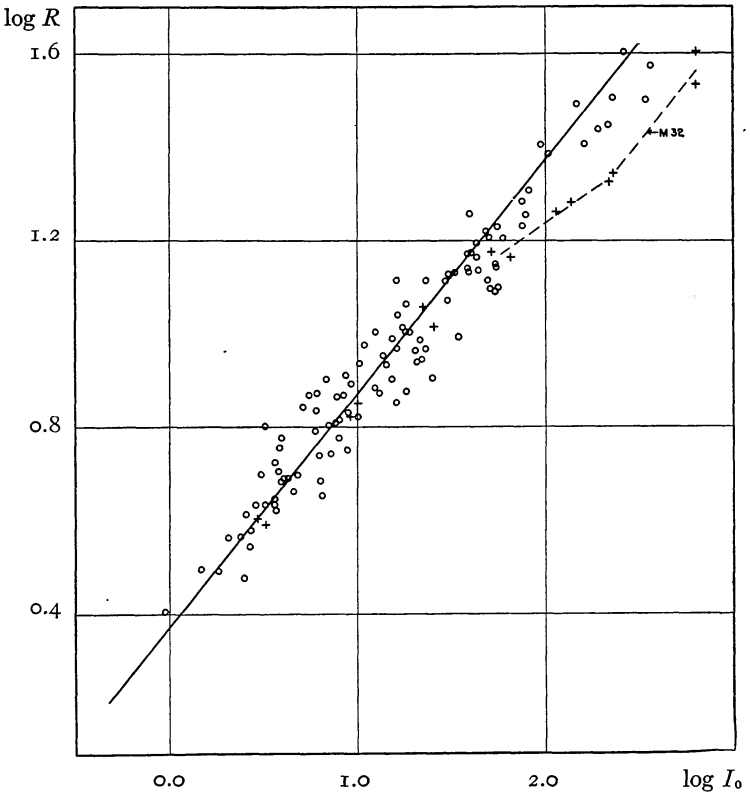

Fig. 6.—Relation between central luminosity and diameter

polation of the intensity scale in Figure 1, namely, $1.058 \times (-0.630) = -0.665$.

In the upper region of the plot most of the points fall below the straight line, a tendency exaggerated by the data for N.G.C. 221 (indicated by crosses), which is superposed on the outer arms of the great spiral, M 31. Its measures may therefore be systematically affected by the luminous background. The marked depression of the points between $\log I_0 = 1.4$ and 1.9 indicates excessive values of $\log I_0$ or deficient values of $\log R$, and hence tends to confirm the observed hump in the corresponding region of the combined luminosity-curve for the long exposures. The remaining high points, however, tend to approach the straight line again rather than to increase the separation. The plot as a whole suggests that formula (3) represents the general trend of the luminosity-curves in the outer regions, but that relatively minor deviations exist which may be significant in the physical interpretation of the curves.

THE SLOPE OF THE TIME SCALES

Results of a similar nature are found in the correlation of diameters with exposure times. The investigation involves, however, the use of the time scales for the plates employed, and, since the necessary data are included in Table VIII, the scales may conveniently be presented at this stage of the discussion and checked against the time scales determined in the laboratory.

The differences between the values of $\log I_0$ for the various images of each nebula represent the displacements of the luminosity-curves due to the different exposure times. They are, in fact, the reduction constants used in combining the various curves of a given nebula. A plot of $\log I_0$ against $\log t$ thus represents the slope of the characteristic time scale of the plates in the form

$$\log I_0 = m_1 \log t + \text{Constant} . \qquad (7)$$

The subscript is used in the coefficient of $\log t$ in order to distinguish it from that in the time scales previously mentioned, where the absorption, A, occurs in place of $\log I$. The relation between the two is, of course, $m_1 = 1.058m$. Since t is expressed in minutes, the con-

stant in formula (7) represents, for a given set of data, the value of log I_0 for an exposure of 1 minute.

In Figure 7, the means of log I_0 for the twenty curves in the first group, representing twelve nebulae, are plotted against log t. The mean of the four values for $t=15$ seconds and the mean of the ten

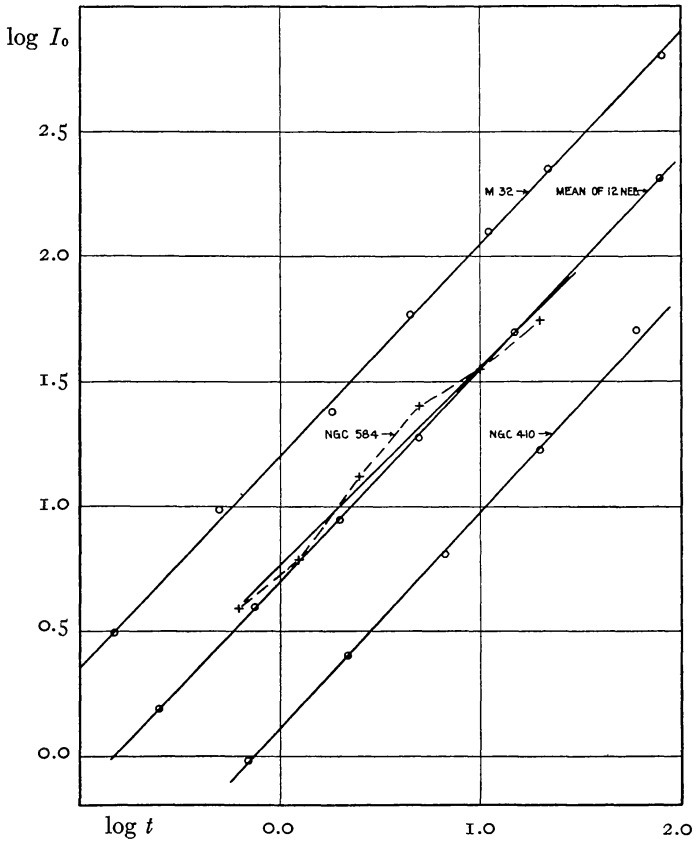

Fig. 7.—Time scales: log $I_0=m_1$ log t+Constant

values for long exposures are corrected by the systematic deviations of these particular curves from the mean curve for the group. The data are well represented by formula (7) with $m_1=0.85$. This corresponds to $m=0.80$, in excellent agreement with the values found in the laboratory. The dispersion among the individual nebulae is satisfactorily small except for a moderate scatter among the points representing the long exposures.

The three plates of N.G.C. 221, with twelve exposures ranging

from 8 seconds to 80 minutes, give the same value, $m_I = 0.85$. The single plate of N.G.C. 410 gives $m_I = 0.87$, and the rather poor single series of N.G.C. 584 may be represented by a line with the slope $m_I = 0.84$. Thus the mean m_I for all the data, 0.85, agrees with the laboratory value, and the deviations among the individual nebulae are unimportant. This is further evidence of the consistency of the data and the validity of the reductions. It also encourages the hope that the luminosity-curves from the long exposures are not altogether unreliable.

CORRELATION OF DIAMETERS AND EXPOSURE TIMES

After this digression on the time scales, the discussion of the correlation between diameters and exposure times may be resumed. From formulae (5) and (7)

$$2 \log R = m_I \log t + \text{Constant} , \qquad (8)$$

where the constant is the difference between the constants in (7) and (5), that is, between $\log I_0$ for an exposure of 1 minute and the threshold value of $\log I$. The data in Table VIII give a separate correlation-curve for each axis of each nebula. The individual curves may be combined by shifting them along the axis of $\log R$ by amounts representing the differences in $\log I_0$ for a given exposure time. In other words, since diameters are functions of central luminosities, the various nebulae may be reduced to a standard central luminosity, and all the data thus collected in a single homogeneous diagram for the comparison of diameters with exposure times.

This has been done in Figure 8. The standard $\log I_0$, as before, is 2.0 for an exposure of 15 minutes, and hence all values of $\log R$ in Table VIII have been corrected by half the difference $2.0 - \log I_0$ (15 min.) in accordance with formula (5). The comparison of this formula with the observations, shown in Figure 6, indicates that errors introduced by the corrections will be of very minor importance.

The data in Figure 8 are fairly well represented by the straight line

$$2 \log R = 0.85 \log t + 1.73 , \qquad (9)$$

which has the slope derived from the time scales. The points for N.G.C. 221, indicated by crosses, show the same systematic discrepancies as in the correlation of log R with log I_0 and may be referred to the same probable source, namely, the luminous background on which the nebula is superposed. Otherwise the most conspicuous discrepancy (the point log $R=0.845$; log $t=-0.602$) refers to the minor axis of the smallest image of the very elongated nebula

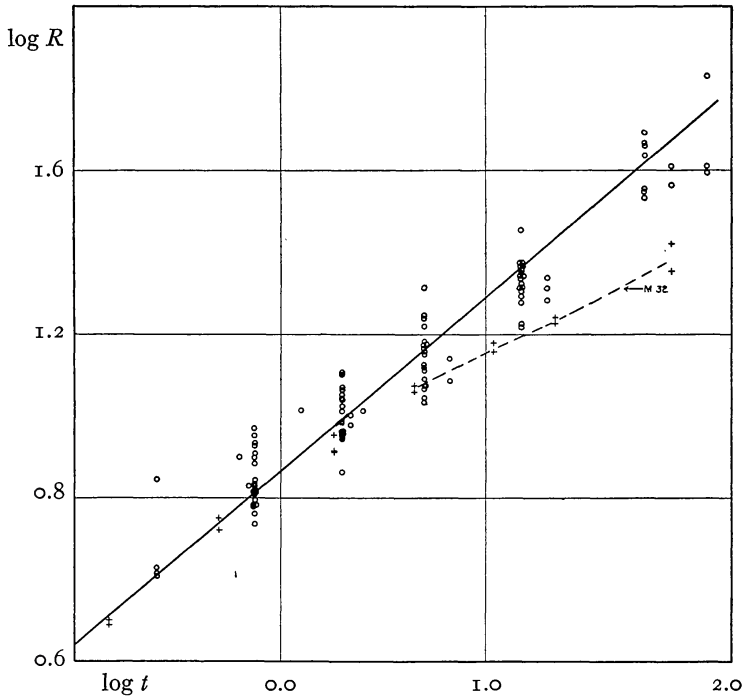

FIG. 8.—Relation between diameter and exposure time

N.G.C. 3115, and hence is entitled to little weight. The slight depression in the region log $t=1.0$ corresponds to that in Figure 6 and to the hump in the mean luminosity-curve for the long exposures.

The constant in formula (9) is the difference between log I_0 for 1 minute, $2.0-(0.851\times0.176)=1.00$, and the threshold value of log I. The latter is therefore -0.73, which is in good agreement with the value in formula (7), namely, -0.74.

The three correlations between the three observed quantities, namely, central luminosities, diameters, and exposure times, are not independent. If any two are found to hold, it follows that the third

also must hold. The correlations involving the diameters, and hence referring to the very threshold of the plates, agree with the luminosity-curves for the long exposures and indicate that formula (3) represents the general trend of the luminosity-curves, without serious systematic divergence, out as far as the observations have been carried.

The correlation between diameters and exposure times, moreover, suggests that the boundaries of the nebulae have not been reached even with the longest exposures. Yet elliptical nebulae appear to be rotating bodies, and hence it is reasonable to assume that some sort of boundary actually does exist. The radii, on such an assumption, must be of the order of $r/a = 35$ or greater.

SIGNIFICANCE OF LOG I

Log I in formula (3) represents surface brightness and hence, within reasonable limits, is independent of the size of the microphotometer slit. The unit, log $I = 0.0$, represents a measured absorption of about 0.116, which is well above the threshold of the plates. The unit varies from plate to plate with the exposure time according to the relation expressing the time scale. The numerical value, as recently determined from extra-focal star images under conditions comparable with those of the nebular plates, appears to be of the order of 19.0 pg. mag. per square second of arc for exposures of 1 minute on Eastman 40 plates. The value varies considerably with the condition of the mirrors, the transparency of the sky, and the sensitivity and development of the plates. Since no precise determinations of these variations were made at the time, the mean value will not give accurate results in individual cases. It is hoped, however, that statistical averages based upon the mean value will be of the proper order of magnitude.

The unit of surface brightness corresponds to a threshold value, log $I = -0.7\pm$, of the order of 20.8 pg.mag. per square second of arc, while the surface brightness of the faintest in-focus star images that can be detected on exposures of 1 minute under the same conditions average about 17.5. Much of this discrepancy is due to the greater ease with which large surfaces can be detected, but, as Seares has pointed out, a portion is probably due to the intermittent exposures

of the vibrating focal images as compared with the continuous exposures for the extra-focal surfaces.[1] The subject is further complicated by the minimum linear dimensions possible in photographic images, and hence the type of telescope may play some rôle. The phenomena affect the determination of total luminosities of nebulae in a very evident manner and indicate the necessity of referring such measures to extra-focal star images comparable in size with the nebular images themselves.

Log I_0 represents the central luminosity on the assumption that the luminosity law holds right up to a point center. The assumption cannot be tested directly because of the spreading of photographic images and the finite area of the photometer slit. It may be noted, however, that most of the luminosity-curves follow the formula up to $2''$ from the center. If the formula held to a point center, the values of log I_0 for curves along the minor and the major diameters of any nebula should be about equal. The data in Table IV indicate, however, that the values for the minor diameters are systematically the larger, the difference increasing with the elongation of the images. The one exception is in the mean curves for N.G.C. 221, which represent the combination of curves from seven images, with a consequent uncertainty in the precise values of the log I_0 finally adopted. Even here the difference, 0.014, is negligible. The mean difference for the other eight nebulae is 0.108.

The discrepancy is partially explained by the observed fact that the ellipticities of isophotal contours increase with distance from the nucleus, at least in the more elongated nebulae—a phenomenon

[1] *Mt. Wilson Contr.*, No. 191, p. 14; *Astrophysical Journal*, **52**, 162, 1920. The threshold value of surface brightness given above represents the mean of measures of fifteen extra-focal exposures on ten nights over a period of six months. It is about 2 mag. fainter than the value given by Seares, based on extra-focal exposures on two nights. A re-examination of the two sets of material, in collaboration with Mr. Seares, indicates a mean difference of the order of 10 per cent in the transparencies of the faintest images. Seares adopted for the threshold images readily detected by the eye, while my estimate was based on the faintest that could be seen under the best conditions, with the thermocouple measures as a guide. On the straight-line portion of the intensity scale, this difference of 10 per cent would correspond to a difference of the order of 0.25 mag., but near the threshold the corresponding magnitude difference is enormously magnified by the asymptotic approaches of the absorption-curve to the axis. This alone is sufficient to account for the divergence in the two estimates of the threshold value, although the influence of observing conditions may also be superimposed.

which will be discussed later. The result is that the luminosity-curves along the minor axis are relatively steeper in the inner region than they would be if the nebulae were precisely symmetrical. Near the nuclei, therefore, the curves must flatten out rather suddenly, as though the luminosity law in all elongated nebulae began to operate at the borders of approximately globular nuclei. The plates themselves show some such phenomenon, for the limiting exposures exhibit round images of uniform density of the order of twice the diameters of the faintest star images. The relatively small variation in the appearance of the nucleus from nebula to nebula, however, is partially due to photographic spreading and to the merging of a surface into a point-source image, and its significance is questionable.

SIGNIFICANCE OF THE PARAMETER a AND THE SYMMETRY OF ISOPHOTAL CONTOURS

The parameter a is the distance from the nucleus at which the luminosity falls to one-fourth of I_0. It is a measure of the luminosity gradient and, after a fashion, of the scale on which the nebula is constructed. If the isophotal contours in the image of an elliptical nebula were all of the same ellipticity, a would vary directly with the radius of any given contour, excepting, perhaps, those very near the nucleus. For an Eo nebula, a would be constant for all diameters. For an elongated nebula, the value of a along any diameter making an angle with the major axis would satisfy the relation

$$a_\phi = \frac{a_{\min}}{\sqrt{1 - e^2 \cos^2 \phi}} . \qquad (10)$$

Expressed in terms of r/a, all the isophotal contours would become circles. This relation has been used in correlating diameters with $\log I_0$ and with exposure times.

The assumption that all isophotal contours in a given image are ellipses with the same eccentricity holds as a first approximation, but further investigation suggests slight systematic deviations among the more elongated nebulae, in the sense that the eccentricity increases with distance from the nucleus. The images of elliptical nebulae appear to be projections of figures of revolution orientated at random, and hence, in the Eo images, representing either globular

nebulae or flattened bodies with their axes of revolution orientated in the line of sight, the contours should be strictly circular. The observational data conform with this interpretation.

E7 nebulae lie at the extreme end of the sequence, and their images are the only ones which can definitely be referred to bodies orientated with their axes of revolution perpendicular to the line of

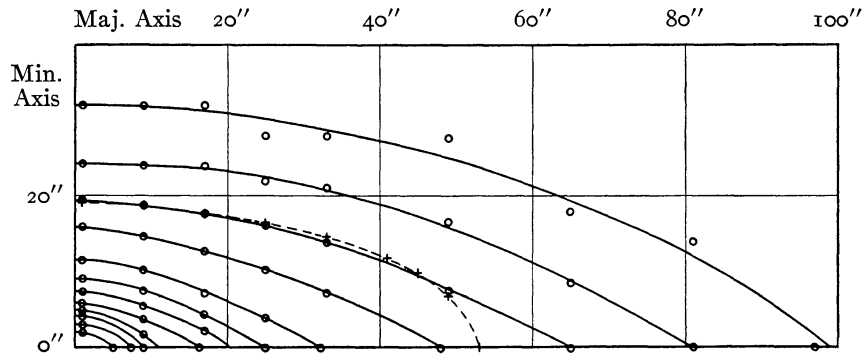

FIG. 9.—Isophotal contours of the image of N.G.C. 3115

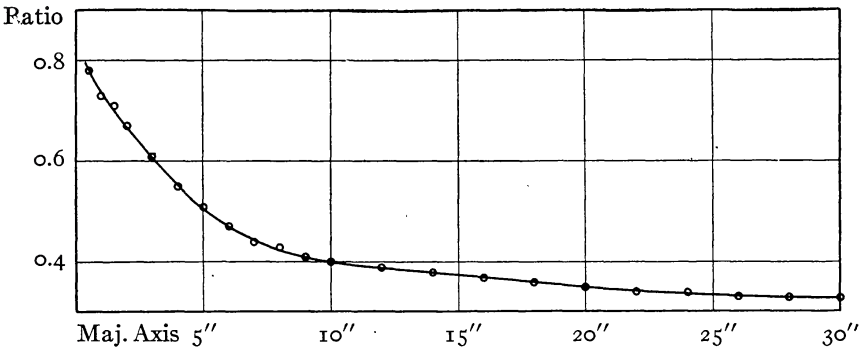

FIG. 10.—Ratios of axes of isophotal contours

sight. Isophotal contours of the type object, N.G.C. 3115 (exposure, 15 min.), have been determined from absorption-curves parallel to the minor axis and cutting the major axis at successive intervals from the nucleus. These contours are shown in Figure 9. They approximate ellipses with the ends drawn out to form the familiar lenticular edge. Although the points very near the nucleus are rather uncertain, the data indicate that the major axis increases faster than the minor, and hence that the outer contours are more elongated than the inner. The reality of this phenomenon is substantiated by com-

paring the luminosity-curves along the two axes of the various images which were combined into the mean curves in Table V. The data are listed in Table IX and are shown graphically in Figure 10. The procedure was as follows. The values of r_{min} were read from the two curves for a given image for values of A corresponding to successive values of r_{maj}. The ratios r_{min}/r_{maj} thus represent the ratio of axes of the successive contours. The results for the various images agree very well except in the nuclear regions of the longer exposures, where the flatness of the measured absorption-curves introduces uncertainties. The ratios diminish steadily from over 0.7 near the nucleus to about 0.33 in the outer regions. The classification E7 is of course based upon long exposures, and refers to the outer contours.

TABLE IX

RATIO OF AXES OF ISOPHOTAL CONTOURS IN IMAGES OF N.G.C. 3115

r Major Axis	Exposure Time					
	15s	45s	2m	5m	15m	Mean
0.5	0.82	0.79	0.75	0.75	0.80	0.78
1	.78	.75	.68	.70	.75	.73
1.5	.79	.73	.70	.68	.63	.71
2	.73	.70	.67	.65	.60	.67
3	.62	.62	.62	.58	.56	.61
4	.58	.56	.56	.54	.54	.55
5	0.54	.51	.53	.51	.48	.51
6	.....	.48	.48	.47	.46	.47
7	.....	.46	.44	.44	.44	.44
8	.....	.44	.43	.42	.42	.43
9	.....	.42	.41	.41	.42	.41
10	.....	0.41	.40	.39	.41	.40
12	.....	.....	.40	.38	.40	.39
14	.....	.....	.39	.37	.39	.38
16	.....	.....	.38	.36	.38	.37
18	.....	.....	.37	.36	.36	.36
20	.....	.....	0.35	.35	.35	.35
22	.....	.....	.....	.34	.35	.34
24	.....	.....	.....	0.34	.34	.34
26	.....	.....	.....	.....	.33	.33
28	.....	.....	.....	.....	.33	.33
30	.....	.....	.....	.....	0.33	0.33

For images intermediate between Eo and E7 the effect varies with the ellipticity. For E1 and E2, it is inappreciable. Isophotal contours of N.G.C. 221 (E2), for instance, are represented by ellipses

within the small errors of observation, out to luminosities of the order of 1 per cent of the central luminosity. In N.G.C. 4382 (E4) and 4621 (E5), the contours deviate very slightly from ellipses in the direction of lenticular figures, the ratio of axes varying from about 0.70 to 0.63 and from 0.64 to 0.56, respectively. The data for the latter two nebulae are considerably less reliable than those for N.G.C. 221 and 3115, but the phenomena appear to be definite, at least in a qualitative sense. Except for the extremely elongated nebulae, however, the deviations of the contours from symmetrical ellipses are so slight that they may be disregarded in general discussions and rough calculations. The present data are not sufficient to examine the range in luminosity gradients among images of a given ellipticity introduced by the projection factor. The most significant evidence bearing on this question is found in the correlation between total luminosities and major diameters.[1]

By integrating formula (3), the total luminosity along any radius is found to be

$$I_0 a^2 \int_0^r \frac{dr}{(r+a)^2} = I_0 a \left(\frac{\frac{r}{a}}{\frac{r}{a}+1} \right). \qquad (11)$$

This of course represents a strip whose width is the unit in which a is expressed. As r/a increases, the total luminosity approaches the simple product $I_0 a$ as a limit. Out to $r/a = 35$, to which the formula probably holds with fair approximation, the total luminosity is over 97 per cent of this product.

TOTAL LUMINOSITIES OF ELLIPTICAL NEBULAE

The total luminosity of the entire nebula out to the distance r/a is found by integrating successive elliptical rings on the assumption that the isophotal contours are all similar ellipses. For the more elongated images this assumption is only an approximation, but, expressed in stellar magnitudes, the deviations are not very serious. The area of an elementary isophotal ring whose semi-minor axis is r

[1] *Mt. Wilson Contr.*, No. 324; *Astrophysical Journal*, **64**, 321, 1926.

and whose width along the minor axis is dr is, neglecting the second-order differential,

$$\frac{\pi}{\sqrt{1-e^2}}\{(r+dr)^2-r^2\}=\frac{2\pi r dr}{\sqrt{1-e^2}}. \tag{12}$$

The luminosity of the ring is this area multiplied by

$$\frac{I_0}{(r/a_{\min}+1)^2}.$$

Integrating these rings out to the distance r along the minor axis, and remembering that $a_{\min}=a_{\mathrm{maj}}\sqrt{1-e^2}$, we find the total luminosity of the nebula to be

$$\left.\begin{aligned} I_t&=\frac{2\pi I_0}{\sqrt{1-e^2}}\int_0^r \frac{r dr}{\left(\frac{r}{a_{\min}}+1\right)^2}, \\ &=2\pi I_0 a_{\min} a_{\mathrm{maj}}\left\{\log_e\left(\frac{r}{a}+1\right)-\frac{\frac{r}{a}}{\frac{r}{a}+1}\right\}. \end{aligned}\right\} \tag{13}$$

The factor within the brackets is independent of the shape of the image and, while the value of a refers formally to the minor axis, that for any radius should lead to approximately the same contour except in the very elongated nebulae. For these the deviations from circularity of the contours, expressed in terms of r/a, introduce an uncertainty as to the proper a to use in the computation, and a similar uncertainty arises in the choice of I_0. More accurate calculations might be based on the assumption of a globular nucleus from the borders of which the luminosity law begins to operate, but for approximate results the mean log I_0 may be used and the deviations from circularity ignored.

The factor within the braces takes care of the exterior regions of the nebula which increasing exposures bring above the threshold of the plate. It depends upon I_0, and both the bracket and I_0 are dependent on the exposure time. The total luminosity derived from a photographic image therefore has little significance except as it is referred to given exposure conditions. The numerical value of the

bracket is unity for $r/a = 5.3 \pm$, which corresponds to a mean exposure of the order of 1 minute for the nebulae considered in the present discussion. The total luminosity is then expressed by the simple formula

$$I_t = 2\pi I_0 a_{\min} a_{\text{maj}} .$$

Total magnitudes are derived from the usual formula

$$m_t = m_c - 2.5 \log I_t ,$$

where m_c is the magnitude per square unit of a for the unit of surface brightness, $\log I = 0.0$. The latter, as previously mentioned, appears

TABLE X

PHOTOGRAPHIC MAGNITUDES CALCULATED FROM DISTRIBUTION OF LUMINOSITY

N.G.C.	m_t $r/a=5.3$	r/a 15^m	m_t		HARVARD		HOLETSCHEK‡ (VISUAL)
			15^m	60^m	I*	II†	
221.....	10.29	20	9.49	9.28	.....	8.7	8.85
410.....	13.44	6	13.35	12.92	.....	.....	.....
584.....	12.49	11	12.00	11.77	.....	11.8	10.9
3115.....	11.32	15	10.66	10.43	.....	9.9	9.5
3379.....	11.47	17	10.75	10.53	.....	10.2	9.4
4278.....	12.10	18.5	11.34	11.12	.....	.....	10.8
4283.....	14.02	17	13.30	13.06	.....	.....	12.2
4374.....	11.92	12.7	11.35	11.10	10.8	.....	9.9
4382.....	11.69	15.0	11.03	10.80	10.9	9.7	10.0
4406.....	11.52	13.7	10.91	10.67	10.9	.....	10.0
4472.....	10.97	14.5	10.33	10.09	10.2	9.1	8.85
4486.....	11.38	8.7	11.03	10.74	10.5	9.2	9.7
4552.....	12.27	11.5	11.81	11.50	11.4	.....	9.9
4621.....	11.91	11.5	11.24	11.00	11.3	.....	10.0
4649.....	11.50	13.3	10.91	10.66	10.5	9.8	9.5

* *Harvard College Observatory Circular*, No. 294, 1926.

† *Proceedings of the National Academy of Sciences*, **15**, 564, 1929.

‡ Revised by Hopman; *Astronomische Nachrichten*, **214**, 425, 1921.

to be of the order of 19.0 mag. per square second of arc for an exposure of 1 minute. Since the unit of a is $2''.03$,

$$m_c = 19.0 + 2.5[0.85 \log t - \log (2.03)^2] ,$$
$$= 20.0 \text{ for } t = 15 \text{ min.}$$

Table X gives total photographic magnitudes for the nebulae here discussed. These have been calculated for exposures of 15 minutes and 1 hour. Magnitudes were first calculated for $r/a = 5.3$ and

then corrected for the observed values of r'/a, i.e., of the observed radius, by means of Table XI, which gives the effect of the bracket in formula (13), expressed in magnitudes, as the images grow with increasing exposure time. This effect is not linear for a given nebula and, moreover, for a given range in exposure time it depends on the central luminosity of the nebula.

For use in Table X the means of $\log I_0$ and of r'/a for the two axes corresponding to the 15-minute exposures have been taken from Tables IV and VIII, except for N.G.C. 221, 410, and 584, for which

TABLE XI

CORRECTIONS TO TOTAL MAGNITUDES OF NEBULAE DEPENDING ON DIAMETERS OF THE IMAGES

r/a	Δm_t*	r/a	Δm_t*
1	+1.78	18	−0.75
2	+0.91	20	.80
3	+ .49	22	.845
4	+ .23	24	.885
5	+ .05	26	.92
5.3	.00	28	.95
6	− .09	30	0.98
7	− .20	32	1.005
8	− .29	34	1.03
9	− .37	36	1.05
10	− .43	38	1.075
12	− .54	40	1.095
14	− .62	45	1.14
16	−0.69	50	−1.17

* $\Delta m_t = 2.5 \log_{10} \left\{ \log_e (r/a+1) - \frac{r/a}{r/a+1} \right\}$.

they have been read from curves relating the two quantities with the exposure times. For N.G.C. 584, for which only one luminosity-curve is available, the values of a for the major and minor axes have been computed on the assumption that the ratio of the two corresponds with the ellipticity of the image.

Table X indicates that the calculated luminosities are of the right order of magnitude, but, in view of the unknown variations in m_c and the approximations involved, very little of further value can be expected from the material. Direct measures of the total photographic magnitudes of nebulae are at present in a very unsatisfactory state. Spirals with fairly definite borders offer less difficulty

than the elliptical nebulae, but in both cases extra-focal images must be used unless the scale of the photographs is so small that the nebulae may be treated as point sources. Even then it will be advisable to investigate the manner in which the photometry of surfaces merges into that of focal star images. In the case of all elliptical nebulae and probably also the earlier-type spirals, the results must be referred to definite exposure conditions and perhaps also to definite instruments.

Published data are too limited for serious discussion. The two lists from Harvard,[1] for instance, have only four nebulae in common, and these show an average difference of more than a magnitude (Table X). The problem is under investigation at Mount Wilson, but very few definite results are as yet available. The standard conditions have been set at extra-focal exposures of one hour with the large reflectors, the plates being measured with a thermocouple; the magnitudes are derived from comparisons with Selected Areas. Preliminary results suggest a systematic difference, for elliptical nebulae at least, between the reflectors and the 10-inch Cooke astrographic camera, while the latter and a Tessar I_c ($f=4.5$) with a focal length of about 10 inches appear to give comparable results. The very few nebulae in the Harvard lists for which definite magnitudes are available at Mount Wilson range from 0.5 mag. fainter (N.G.C. 1700) to 1.5 mag. brighter (N.G.C. 7619) than the Harvard values. This illustrates the necessity for careful investigation before a system of photographic magnitudes can be adopted.

DISTRIBUTION OF LUMINOSITY IN ELLIPTICAL NEBULAE

Since formula (3) appears to give a reasonable approximation to the distribution of luminosity in the projected images, it is of considerable interest to examine the corresponding distribution in the nebulae themselves. The absence of conspicuous flattening of luminosity-curves in the central regions suggests that absorption of light is inappreciable. This is in line with the more definite evidence from novae and Cepheids involved in the nuclear region of M 31.[2] Scatter-

[1] *Harvard College Observatory Circular*, No. 294, 1926, and *Proceedings of the National Academy of Sciences*, **15**, 564, 1929. Both lists purport to give photographic magnitudes on the international scale.

[2] *Mt. Wilson Contr.*, No. 376; *Astrophysical Journal*, **69**, 103, 1929.

ing may also be neglected, for plates exposed through a visual color filter show no difference in color between the nuclei and the outer regions of elliptical nebulae. The conditions may be further simplified by considering the case of a globular nebula and assuming, as a first approximation, that the empirical formula holds indefinitely. The problem then becomes analogous to that of determining the distribution of stars in a globular cluster from star counts, as discussed by Plummer, von Zeipel, and many others. The solution of an integral equation leads to the following relation,[1]

$$f(\rho)=-\frac{1}{\pi}\int_{\rho}^{\infty}\frac{F'(r)dr}{\sqrt{r^2-\rho^2}}, \tag{14}$$

where $f(\rho)$ represents the distribution of luminosity in the three-dimensional nebula as a function of distance ρ from the nucleus, and $F(r)$ the observed distribution in the projected image, namely, formula (3) or its equivalent, formula (4). On introducing the derivative of (4), the relation becomes

$$f(\rho)=\frac{2I_0a^2}{\pi}\int_{\rho}^{\infty}\frac{dr}{(r+a)^3\sqrt{r^2-\rho^2}}. \tag{15}$$

This expression can be integrated directly[2] although the procedure is rather clumsy. The three cases in which ρ is less than, equal to, and greater than a must be solved separately. The solutions are

Case I: $\rho=a$

$$f(\rho)=\frac{4I_0}{15\pi a},$$

Case II: $\rho<a$

$$f(\rho)=-\frac{I_0a^2}{\pi(a^2-\rho^2)^2}\left\{3a-\frac{3a^2-(a^2-\rho^2)}{\sqrt{a^2-\rho^2}}\log_e\frac{a+\sqrt{a^2-\rho^2}}{\rho}\right\},$$

Case III: $\rho>a$

$$f(\rho)=-\frac{I_0a^2}{\pi(a^2-\rho^2)^2}\left\{3a-\frac{3a^2-(a^2-\rho^2)}{\sqrt{\rho^2-a^2}}\left(\tan^{-1}\frac{-a}{\sqrt{\rho^2-a^2}}+\frac{\pi}{2}\right)\right\}.$$

[1] Details of the solution will be found in the several articles on the distribution of stars in globular clusters. See, for instance, H. C. Plummer, *Monthly Notices of the Royal Astronomical Society*, **71**, 460, 1911.

[2] Pierce, *A Short Table of Integrals*, Nos. 195, 196, 205, 206.

Let $z_1 = 1 - (\rho/a)^2$ and $z_2 = -z_1 = (\rho/a)^2 - 1$; then, neglecting the constant $I_0/\pi a$, which appears as a coefficient in each case, we find

$$\text{Case I:} \quad f(\rho) = 4/15 ,$$

$$\text{Case II:} \quad f(\rho) = \frac{1}{z_1^2}\left\{\frac{3-z_1}{\sqrt{z_1}} \log_e \frac{1+\sqrt{z_1}}{\sqrt{1-z_1}} - 3\right\}, \tag{16}$$

$$\text{Case III:} \quad f(\rho) = \frac{1}{z_2^2}\left\{\frac{3+z_2}{\sqrt{z_2}}\left(\tan^{-1}\frac{1}{\sqrt{z_2}} + \frac{\pi}{2}\right) - 3\right\}. \tag{17}$$

The formulae express the distribution of luminosity in the three-dimensional nebula as a function of ρ/a where a is the same quantity

TABLE XII

DISTRIBUTION OF LUMINOSITY IN ELLIPTICAL NEBULAE

ρ/a*	$I = f(\rho/a)$*	log 100 I	ρ/a*	$I = f(\rho/a)$*	log 100 I
0.0	.....	.....	3.5	0.0193	0.286
0.05	4.44	2.647	4	.0142	0.152
.1	3.108	2.493	5	.00790	9.898
.2	1.924	2.284	6	.00491	9.691
.3	1.335	2.126	8	.00227	9.356
.4	0.981	1.992	10	.00123	9.090
.5	.750	1.875	12	.000741	8.870
.6	.588	1.769	15	.000394	8.594
.8	.383	1.583	20	.000173	8.238
1.0	.267	1.426	25	.0000910	7.959
1.2	.194	1.288	30	.0000535	7.728
1.5	.126	1.100	40	.0000230	7.362
2.0	.0697	0.843	50	.0000119	7.076
2.5	.0425	.628	70	.00000442	6.645
3	0.0279	0.446	100	0.00000154	6.187

* ρ/a represents distance from the center of the three-dimensional nebula. The units of both distance and luminosity are arbitrary.

as in formula (3). Table XII gives numerical values of $f(\rho/a)$, which are proportional to the luminosity, for successive values of ρ/a, and Figure 11 shows the luminosity-curve plotted as a relation between log I and log ρ/a.

COMPARISON OF LUMINOSITY DISTRIBUTION IN NEBULAE WITH DENSITY DISTRIBUTION IN AN ISOTHERMAL GAS SPHERE

The complexity of formulae (16) and (17) doubtless arises from the introduction of an empirical formula into an integral equation. The formula, moreover, is assumed to hold from 0 to ∞, although there is reason to suppose that it is not valid for very small values,

say $r/a < 0.25$, and that it cannot be followed indefinitely. The luminosity-curve in Figure 11 can therefore be accepted only as a first approximation for comparison with other curves whose significance is known.

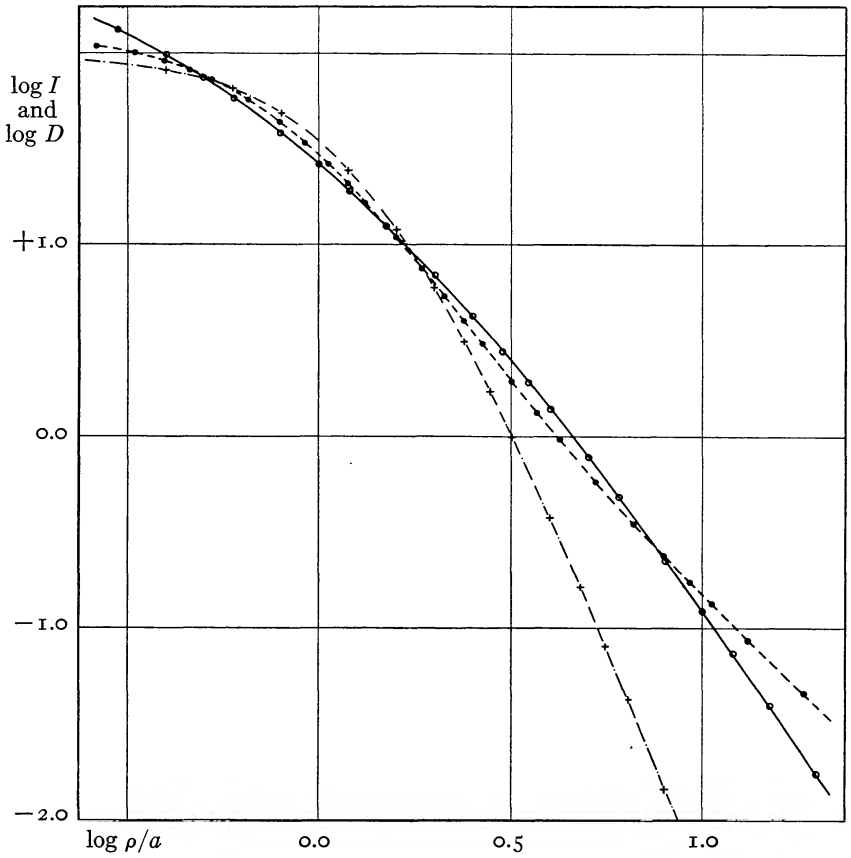

FIG. 11.—Luminosity distribution in globular nebulae (circles) compared with density distribution in an isothermal gas sphere (dots) and with stellar distribution in a globular cluster (crosses).

One such comparison, based on the assumption that distribution of luminosity represents distribution of mass, is with the density distribution in an isothermal gas sphere as computed by Emden in his well-known *Gaskugeln* (Tabelle 14). This also is shown in Figure 11 in the form $\log r_1 = f(\log p_1)$, r_1 and p_1, in Emden's notation, signifying distances from the center and densities, respectively. The curve has been shifted into approximate coincidence with the lumi-

nosity-curve by adding -0.58 to log r_1 and $+2.11$ to log p_1. The third curve in Figure 11 represents the density distribution in an adiabatic gas sphere of class $n=5$, $k=6/5$ (Emden, Tabelle 11), and is included because it approximates in a general way the distribution of stars in a globular cluster, and hence emphasizes the wide difference between these objects and the elliptical nebulae.

The luminosity-curve falls well above both density-curves in the immediate neighborhood of the center, say $\rho/a<0.25$, thus indicating more highly concentrated nuclei in the nebulae. From this point out to $\rho/a=10$ or 11 (isothermal density $=0.001$ central density) the luminosity-curve follows the isothermal density-curve rather closely, but from there outward it deviates systematically from the latter in the general direction of the adiabatic curve. The isothermal sphere extends to infinity and has infinite mass. The nebulae, on the other hand, appear to be rotating bodies, and hence infinite dimensions can scarcely be attributed to them. If we admit the analogy throughout the central region, outside of the nucleus itself, the luminosity-curve would therefore be expected to deviate from the density-curve in the outer regions in the direction actually observed, namely, toward that of finite dimensions, or of the system which Emden calls *isotherm-adiabatische.*

The similarity of the two distribution laws over the central region is confirmed when the isothermal gas sphere is projected on a plane and the projected density distribution is compared with the luminosity distribution actually observed in the nebular images. This comparison evades the assumptions introduced in deriving the luminosity law for the three-dimensional nebula. The projection may be made graphically by constructing density-curves along parallel lines at successive distances from the center and then plotting the areas under these curves against the distances. Since the densities in the extreme outer regions tend to follow the inverse-square law, the areas are finite and may be estimated to approximations sufficient for the present purpose. Results for such a solution are given in Table XIII, although no great accuracy can be assigned to the numerical values. In Figure 12 the projected density-curve is compared with the observed luminosity-curve.

The comparison indicates that the nuclear luminosity is definitely more concentrated than the central density of the gas sphere; that, from about $\rho/a = 0.5$ to 5.0, the two distribution-curves agree fairly well; that beyond 5.0 the luminosity-curve falls increasingly below the density-curve, as would be expected from the finite dimensions of the nebula.

TABLE XIII

PROJECTED DENSITIES IN THE ISOTHERMAL GAS SPHERE

r_1	D	log D	log $(D-30)$
0	3032	3.482	+3.477
0.5	2962	3.472	3.467
1	2729	3.436	3.431
1.5	2430	3.386	3.380
2	2106	3.324	3.317
3	1524	3.183	3.174
4	1103	3.042	3.031
5	832	2.920	2.904
6	649	2.812	2.792
7	522	2.718	2.692
8	430	2.633	2.602
9	366	2.563	2.526
10	318	2.502	2.459
12	254	2.404	2.350
14	210	2.323	2.255
16	179	2.252	2.173
18	157	2.197	2.104
20	140	2.147	2.041
25	111	2.045	1.908
30	92.0	1.964	1.792
40	69.6	1.843	1.598
50	56.5	1.752	1.423
70	41.5	1.618	+1.061
100	30.2	1.480	−0.699
150	21.1	1.324	.....
200	16.3	1.213	.....
300	10.9	1.038	.....
500	6.5	0.814	.....

The order of the discrepancies is indicated when arbitrary boundaries are assigned to the gas sphere out to which Emden's curve is assumed to hold, and the bounded spheres are projected on to a plane. A very good agreement is found when the limit is set at $r_1 = 100\pm$, where the density in the gas sphere is of the order of 0.0002 of the central density and that in the projection about 1 per cent of the projected central density. The projected densities for the bound-

ed sphere are derived with a fair approximation, except near the boundary, by subtracting a constant from the projected densities for the unbounded sphere. For the present purpose the constant has been selected as 30 units, corresponding to the projected density in

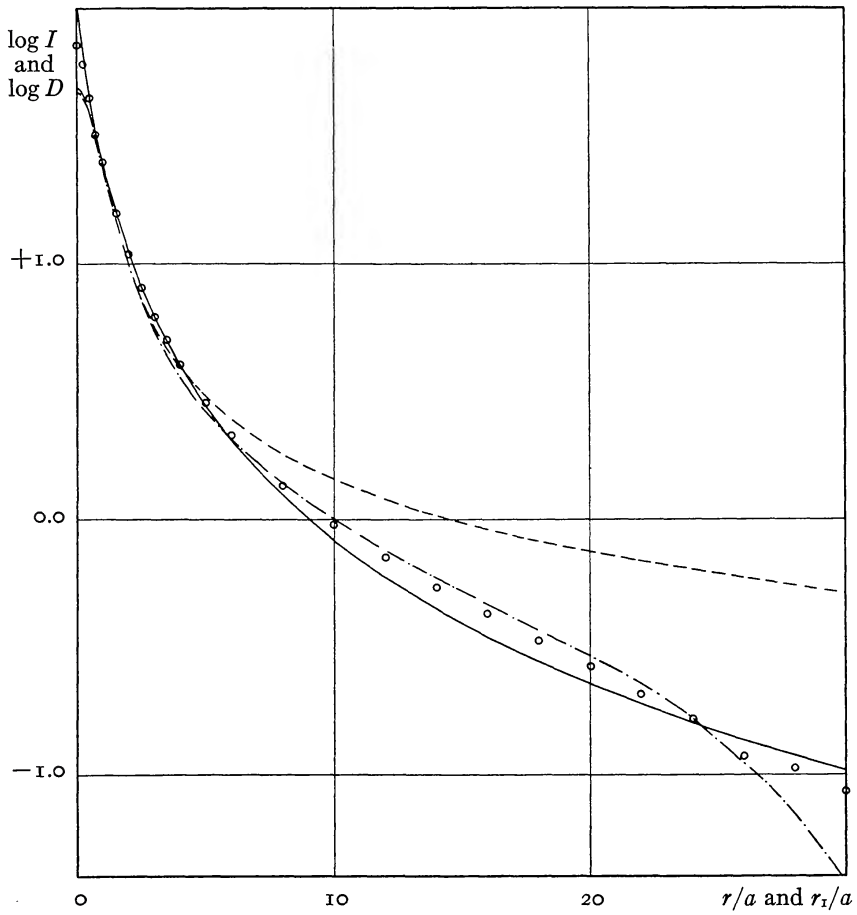

FIG. 12.—Comparison of luminosity distribution in the projected images of elliptical nebulae (full line, formula [3]) with density distribution in the projection of an isothermal gas sphere (dashes) and a bounded gas sphere (dash-dot). The circles represent the measured luminosities on long exposures shown in Fig. 5.

the unbounded sphere at about $r_1 = 101$, and the results of the operation are listed in the fourth column of Table XIII.

These data are represented approximately by a formula similar to (3),

$$\log D = \log D_0 - 2 \log (r_1/a + 1) ,$$

where a is 3.0 and $\log D_0$ is about 3.79, which also holds for the central region of the projection of the unbounded sphere.

Figure 12 gives four curves, representing, respectively, formula (3), the observed luminosity-curve from the long exposures, the density-curve for the projection of the unbounded gaseous sphere, and the density-curve for the projection of the bounded gaseous sphere. The observations fall between the first and last curves, with little choice between them except at the center and in the extreme outer region where the measures have little weight. The deviations of the measures from formula (3) in the interval $r/a = 8$ to 22 represent the hump in the luminosity-curve for long exposures mentioned in a previous paragraph and are in the direction of the bounded gaseous sphere. The latter, moreover, has a radius of the order of $r_1/a = 34 \pm$ which is comparable with the radii observed in the longer exposures of the nebulae. The comparison with the arbitrarily bounded gaseous sphere has no definite physical significance, but it serves to emphasize the similarity between luminosity distribution in the nebulae and density distribution under isothermal conditions, which is partially masked by the infinite dimensions of the complete gaseous sphere.

Further consideration of the problem here raised has no part in the present investigation, which is essentially a presentation of the data of observations. It is hoped that they may furnish an observational basis for the dynamical study of elliptical nebulae.

CARNEGIE INSTITUTION OF WASHINGTON
MOUNT WILSON OBSERVATORY
February 1930